Automatic identification of ischemia using lightweight attention network in PET cardiac perfusion imaging

Muhammad Hassan Nawaz

Master´s thesis

Abo Akademi University
Faculty of Science and Engineering
08.06.2023

Master´s degree in Biomedical Imaging

Credits: 40 ECTS

Supervisors:

1. Prof. Abdulhamit Subasi
   Professor (Department of Biomedicine and Medical Physics, University of Turku)
   abdulhamit.subasi@utu.fi

2. Prof. Riku Klén
   Assistant Professor (Imaging instrumentation and detection technologies, University of Turku, Turku PET Centre)
   riku.klen@utu.fi

Abstract

ABO AKADEMI UNIVERSITY
Department of Biosciences
Faculty of Science and Engineering

MUHAMMAD HASSAN NAWAZ :
Automatic identification of ischemia using lightweight attention network in PET cardiac perfusion imaging

Master's thesis, 71 pp.
Biomedical Imaging
June, 2023

Ischemic disease, caused by inadequate blood supply to organs or tissues, poses a significant global health challenge. Early detection of ischemia is crucial for timely intervention and improved patient outcomes. Myocardial perfusion imaging with positron-emission tomography (PET) is a non-invasive technique used to identify ischemia. However, accurately interpreting PET images can be challenging, necessitating the development of reliable classification methods. In this study, we propose a novel approach using MS-DenseNet, a lightweight attention network, for the detection and classification of ischemia from myocardial polar maps. Our model incorporates the squeeze and excitation modules to emphasize relevant feature channels and suppress unnecessary ones. By effectively utilizing channel interdependencies, we achieve optimum reuse of interchannel interactions, enhancing the model's performance. To evaluate the efficacy and accuracy of our proposed model, we compare it with transfer learning models commonly used in medical image analysis. We conducted experiments using a dataset of 138 polar maps (JPEG) obtained from 15O_H2O stress perfusion studies, comprising patients with ischemic and non-ischemic condition. Our results demonstrate that MS-DenseNet outperforms the transfer learning models, highlighting its potential for accurate ischemia detection and classification. This research contributes to the field of ischemia diagnosis by introducing a lightweight attention network that effectively captures the relevant features from myocardial polar maps. The integration of the squeeze and excitation modules further enhances the model's discriminative capabilities. The proposed MS-DenseNet offers a promising solution for accurate and efficient ischemia detection, potentially improving the speed and accuracy of diagnosis and leading to better patient outcomes.

KEYWORDS: PET Imaging, CNN, Transfer Learning, MS-DenseNet, Ischemia.

List of Abbreviations

AI	Artificial intelligence
AdaBoost	Adaptive boosting
CT	Computed tomography
CAD	Computer-aided diagnosis
CNN	Convolutional neural network
CMR	Cardiac magnetic resonance
CTA	Computed tomography angiography
DL	Deep learning
DWSC	Depthwise separable convolution
EHR	Electronic health record
FC	Fully connected
FFR	Fractional flow reserve
GAP	Global average pooling
ICA	Independent component analysis
k-NN	k-nearest neighbours algorithm
LDL	Low-density lipoprotein
MS-DenseNet	Multi-scale dense network
MRI	Magnetic resonance imaging
MPI	Myocardial perfusion imaging
ML	Machine learning
MLP	Multi-layer perceptron classifier
NMF	Non-negative matrix factorization
NLP	Natural language processing
PET	Positron emission tomography
PCA	Principle component analysis
ROI	Region of interest
SVM	Support vector machines
SPECT	Single photon emission computed tomography
SE	Squeeze and excitation
TL	Transfer learning
XGBoost	Extreme gradient boosting
2D-OSEM	The two-dimensional ordered expectation-maximization algorithm

Table of Contents

1. LITERATURE OVERVIEW

1.1. Introduction

This thrilling era, which many have dubbed the "Information Age" to reflect the exponential growth of available data, is truly remarkable. The visual data has also increased dramatically, with a rise in both videos and images. Around 300 hours of YouTube videos get uploaded online every minute, and that's just a fraction of the total amount of media created each year. Information on healthcare is being generated at an exponential rate and analyzed for insights every second. The healthcare sector currently accounts for roughly 30% of global data volume. By 2025, the CAGR (compound annual growth rate of data) of healthcare data would have reached 36% [1]. That's a rate that's 11% quicker than the media and entertainment industry and 10% faster than the financial services industry [1].

It is not possible for humans to keep up with the exponential growth of data, so researchers are constantly looking for machine-based solutions to the problem of data classification. Computer vision, an interdisciplinary area that studies how computers acquire knowledge of digital images, is responsible for automatic image-based data analysis (which also includes medical data). The goal of computer vision is to automatically do activities that human and animal visual systems can. Classification, detection, and segmentation are typical applications of image analysis [2]. The goal of the algorithm in the classification challenge is to divide an image into two or more distinct categories. Lung nodules, for instance, can be categorized as benign or malignant, and visuals can be sorted into those with cats and those with dogs. The purpose of the algorithm in the detection task is to locate objects in 2D or 3D space, such as the identification of lung nodules in Computed Tomography (CT) scans. The algorithm's goal in the segmentation challenge is to provide a pixel-wise delineation of pathology or an organ, such as the surface of a lung, kidney, spleen, or tumor in a CT, ultrasound, or Magnetic Resonance Imaging (MRI) image.

In this thesis, we apply transfer learning to a medical problem of practical importance—the classification of images from nuclear imaging for the diagnosis of myocardial ischemia—at

the interface of medicine and computer science. This research has the potential to improve the accuracy and efficacy of healthcare diagnosis by shedding light on how transfer learning might be implemented in real-world procedures.

This thesis is broken down into five sections: the introduction, the ischemia heart disease, the artificial intelligence, the materials and methods, the experimental results, the discussion and the conclusion. As a whole, the thesis starts with an explanation of the issue and the suggested solution, moves on to the execution, and then discusses the outcomes. Each section of the thesis will be organized as follows.

The most important ideas presented in this thesis are outlined in the Introduction/Literature Overview (Chapter 1). The purpose of this chapter is to expose the reader to the study's basic principles, as well as its primary themes and overarching goals. This chapter focuses on the organization of the thesis, the identification of the issue, and the placement of the solution. Artificial intelligence and myocardial ischemia are two of the major concepts that are defined in literature overview. Furthermore, the purpose of this chapter is to offer empirical proof that the stated issue is indeed a serious one. Finally, it tries to explain why this study is an important addition to the field and how it builds on earlier findings. Data collection and pre-processing specifics for this study are included in Materials and Methods (Chapter 2), along with the overall workflow of ischemia detection from polar maps. The outcomes of this study and potential future research topics are covered in Results and Discussion (Chapters 3-4). Finally, we concluded the findings of our thesis in Chapter 5.

1.2. Motivation

Heart disease has been a leading cause of mortality and disability worldwide over the past three decades. One-third of all fatalities in 2019 were attributable to the disease, which includes stroke and heart attack [3]. Research published in the journal Circulation found that deaths from cardiovascular disease rose during the pandemic, affecting Hispanic, Black, and Asian individuals disproportionately [4]. An analysis of fatalities in the United States from March-August 2020 found that 339,076 were caused by cardiovascular disease and 76,767 were caused by cerebral artery disease, which affects the brain's vascular system [3].

Consequently, cardiac diseases must be addressed and managed carefully which also includes myocardial ischemic condition. This is why high-tech imaging methods like nuclear imaging are so important for early identification of potentially fatal diseases. Positron Emission Tomography (PET) imaging and other nuclear imaging methods have received a lot of headlines lately for their potential to aid in the detection of myocardial ischemia [5]. The interpretation or analysis of images acquired by PET-MPI (Myocardial Perfusion Imaging) is generally undertaken by medical professionals. Clinical interpretations can be greatly improved by using AI-enhanced computer-aided diagnosis (CAD) tools [6] [7]. Furthermore, AI techniques can be beneficial in some jobs, such as image classification in medicine, a crucial issue to identify diseases. For instance, making a diagnosis of cardiac ischemia using polar map image-data is fundamentally a classification problem. In these situations, doctors need to determine if a given polar map shows a normal (high perfusion) or abnormal (low perfusion) state of health [5] [8].

Deep learning, the subfield of machine learning that makes use of multilayered neural networks, has attracted a lot of attention in recent decades. With the help of convolutional neural networks (CNN), deep learning has achieved remarkable success in image-based data classification and analysis tasks. In the field of medical imaging research, numerous effective classification algorithms have been implemented using machine learning approaches [9] [10] [11]. Many medical professionals have heard of and used successful classifiers like the support vector machine (SVM) and k-nearest neighbor (k-NN) [12] [13]. Deep learning (DL) has been the method of choice recently for solving previously intractable problems and significantly improving the performance of traditional machine learning methods. Furthermore, DL is not a specialized approach; rather, it is a disruptive force in many other scientific areas. Researchers in the field of medical imaging must thus immediately and fully use DL technology.

CNNs have quickly risen to prominence as one of the most widely used methods for image classification since the 2012 ImageNet competition [14]. Therefore, researchers in the field of medical imaging have looked to CNNs to help them with medical image classification

problems so that doctors may make more informed diagnoses [15]. Simply said, a CNN is a prediction model which analyzes and categorizes images by feeding with a large training dataset [16]. CNNs have shown promising results in many areas, but they have yet to be widely embraced for use in medical image classification problems, where real-world data is typically scarce and computational resources are expensive. Ethical concerns can arise when attempting to gain access to medical records stored in bioinformatics facilities [15] [17]. The difficulties of creating a unique CNN can also be met through the use of transfer learning. Predictive capability of a CNN model trained on a huge dataset can be leveraged on new tasks [18] [19] [20]. This technique is known as Transfer Learning (TL). The performance and effectiveness of DL in classification problems is enhanced by transfer learning, according to a number of published research [21]. Since these pre-trained models were developed for use with natural data, applying them to the classification of medical images remains an intriguing and difficult area of study [22].

1.3. Previous Studies in Ischemia Diagnosis

There have been several notable studies related to ischemia detection from polar maps and classification using transfer learning and machine learning. In this section, we will summarize key studies related to our work as shown in Table 1.

Table 1. Previous studies found in ischemic detection.

Ref.	***Applications***	***Clinical Interpretation***	***Custom CNN***	***TL***	***ML***	***MS-DenseNet***	***Best Accuracy***
[7]	Ischemia Detection				✓		**71-72%**
[23]	Ischemia Detection	-	✓	-	✓	-	Upto 88%
[24]	Ischemia Detection	✓	✓	-	-	-	83%
[25]	Ischemia Detection	-	-	✓	-	-	86%
[26]	Ischemia Detection		✓	✓			**82%**
[27]	Myocardial Infarction		✓				**93-95%**
[28]	Ischemia Detection		✓				**94-95%**
Our work	**Ischemia Detection**	**-**	**-**	✓	✓	✓	**97%**

Klen et al. [23] demonstrated the potential of machine learning in detecting myocardial ischemia using polar map data from PET myocardial perfusion imaging. The authors compared various ML algorithms, including logistic regression (LR), support vector

machines (SVM), and random forests (RF), and reported a (0.75-0.88) accuracy score with 10-fold cross-validation and (0.70-0.87) accuracy score with a separate holdout dataset.

Teuho et al. [24] applied custom CNN to polar map data for automatic detection of myocardial ischemia. They compared CNN-based methods for detecting ischemia with clinical interpretation. CNN based model achieved 83% accuracy. However, it was 5% less than the accuracy of clinical interpretation which is 87%.

Seyed et al. [25] presented various transfer learning models for automatic detection of ischemia from polar maps. In this study, the VGG19 model achieved 85% accuracy which is 2% higher than that of custom CNN model presented by Teuho et al. [24]. The accuracy was further improved to 86% by incorporating ensemble learning in Seyed et al. study.

For ensemble learning ML, 16 features were used in the study of Luis Eduardo et al. (2018) [7]. ML identified patients with myocardial ischemia and those at increased risk of MACE with accuracies of 0.72 and 0.71, respectively. In another study (2020), Luis et al. implemented DL architecture based on transferred layers from the neural network of ResNet50. DL showed accuracy at 82% with sensitivity around 87% [26].

In 2017, Acharya et al. focused on automatic detection of myocardial infarction using convolutional neural network [27]. Using ECG beats with and without noise removal, this study's average accuracy was 93.53% and 95.22 percent, respectively. Another study found that Deep CNN had an acc of 94.95% for segment 1 (2 seconds) and 95.11% for segment 2 (5 seconds) when determining whether or not an ECG was normal or abnormal [28].

1.4. Ischemia Heart Disease

Insufficient blood and oxygen delivery to the heart muscle is the hallmark of myocardial ischemia, a medical condition typically caused by the blockage or constriction of coronary arteries. In this section, we discussed etiology, pathophysiology, and clinical manifestations of myocardial ischemia as follows:

1.4.1. Etiology

Myocardial infarction, sudden cardiac death, and angina are just a few of the potentially serious side effects of myocardial ischemia, a pathological state that develops when the flow of oxygenated blood to the heart muscle is insufficient as shown in Figure 1. Myocardial ischemia is caused by a complex combination of environmental, genetic, and behavioural variables, which has a multifactorial etiology. This thorough analysis goes into great detail into the causes of myocardial ischemia.

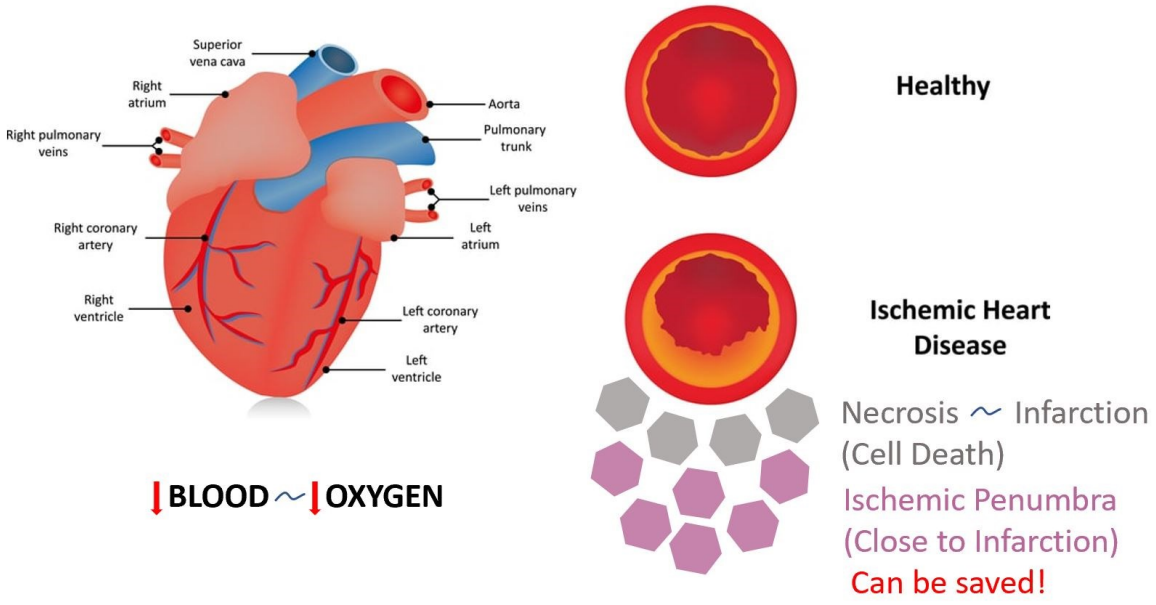

Figure 1. Ischemic heart condition caused by infarction or insufficient oxygenated blood flow.

a) Atherosclerosis

The main factor causing myocardial ischemia is atherosclerosis [29]. It is a long-lasting inflammatory condition that causes atherosclerotic plaques to form in the artery walls as a

result of the slow buildup of inflammatory cells, lipids, and fibrous tissue. These plaques can obstruct the coronary arteries completely or partially, which would reduce blood flow to myocardium. A number of processes contribute to atherosclerosis development:

- Endothelial dysfunction: The onset of atherosclerosis is marked by endothelial dysfunction. Reduced ability to vasodilate, increased vascular permeability, pro-inflammatory, and pro-thrombotic states are its defining characteristics [30]. Endothelial dysfunction can be caused by many things, including smoking, high blood pressure, hyperlipidemia, and diabetes mellitus.
- Lipid accumulation: Low-density lipoprotein (LDL) particles that are carrying cholesterol infiltrate and become entrapped in the artery intima. Oxidized LDL (extremely atherogenic) is created when these particles go through oxidative alteration. By stimulating endothelial, smooth muscle, and macrophage cells, oxy-LDL can cause an inflammatory response.
- Plaque and inflammation development: Activated endothelial cells release adhesion molecules, which promote the attraction of circulating leukocytes, especially monocytes, to the artery intima. Monocytes change into macrophages once they reach the intima, which absorbs ox-LDL particles and develops into lipid-rich foam cells. Foam cell buildup, smooth muscle cell division, and extracellular matrix synthesis all contribute to the development of atherosclerotic plaques.
- Plaque development and complications: Atherosclerotic plaques can advance to induce luminal constriction, which lowers blood flow and causes myocardial ischemia. Plaques that have thin fibrous cap, a substantial necrotic core, and a significant amount of inflammatory cells are thought to be weak and more prone to rupturing. Acute coronary events, e.g. myocardial infarction, and thrombus development are both caused by plaque rupture.

b) Coronary artery vasospasm

Vasospasm, or sudden and temporary constricting of coronary arteries, can result in myocardial ischemia by limiting the flow of blood to myocardium [31]. Vasospasm can happen on its own or be brought on by things like being exposed to the cold, going through

stressful situations, or using cocaine. Endothelial dysfunction, an increase in the generation of vasoconstrictor chemicals, and improved cardiovascular smooth muscle contractility are all factors in the underlying mechanism of vasospasm.

c) Thromboembolic events

These events are yet another potential factor in myocardial ischemia. The development of blood clots can take place outside of or inside the coronary arteries, with the clots then having the potential to embolize coronary circulation. Thrombi can develop as a result of endothelium damage, hypercoagulable states or blood stasis, which can result from genetic factors, acquired diseases, or the use of particular drugs [32].

d) Structural abnormalities

The occurrence of myocardial ischemia can be attributed to the modification of blood flow and the hindrance of oxygen supply to heart muscle, which can be caused by structural anomalies of the coronary arteries, whether they are congenital or acquired [33]. Congenital anomalies are infrequent occurrences; however, they can have notable impacts, especially among the younger population. The aforementioned instances comprise single coronary artery, anomalous coronary artery origin, and coronary artery fistula, that may result in compromised blood supply and ischemia.

The development of coronary artery anomalies can be attributed to a range of factors including pathological conditions, physical injury, or medical procedures. Coronary artery dissection is a medical condition characterized by a breakdown of arterial wall layers, leading to the obstruction of blood flow and consequent ischemia. During cardiac operations e.g. percutaneous coronary intervention or coronary artery bypass grafting, iatrogenic coronary artery injuries may arise, resulting in compromised blood flow or adverse effects such as dissection, thrombosis, or restenosis. Kawasaki disease is a type of acute systemic vasculitis that primarily affects young children. It has the potential to cause coronary artery aneurysms, occlusions or stenosis, which can lead to myocardial ischemia or infarction.

1.4.2. Pathophysiology

Myocardial ischemia is a condition characterized by insufficient delivery of oxygen to the heart muscle, also known as myocardium, resulting from a decrease or constriction of blood

flow. The pathophysiological mechanisms underlying myocardial ischemia are intricate and multifactorial, encompassing a cascade of interrelated processes that culminate in cellular impairment and consequent injury to the myocardial tissue [34].

Myocardial ischemia is primarily caused by a discrepancy between the supply and demand of oxygen in the myocardium. The phenomenon can manifest due to various factors, such as heightened myocardial workload, diminished blood oxygen-carrying capacity, or a confluence of both. Coronary blood flow is the primary determinant of oxygen supply to the heart muscle. However, this flow can be negatively impacted by various factors, including vasospasm, atherosclerosis or thromboembolic events. In contrast, the determination of myocardial oxygen demand is contingent upon various factors, including contractility, heart rate, and wall stress. Ischemia occurs when the myocardium's oxygen demand surpasses the available supply [35] [36].

Myocardial cells experience a lack of oxygen during an ischemic period, which results in their inability to sustain aerobic metabolism. Consequently, individuals transition to anaerobic metabolism, resulting in a reduced energy production rate and the buildup of hydrogen ions and lactate. The alteration in metabolic processes causes a reduction in the pH within the cell, thereby compromising its functionality and initiating a series of deleterious consequences on the myocardium [37].

The presence of hydrogen ions and lactate in ischemic myocardium can initiate various cellular processes, such as hindrance of ion transportation through the cell membrane, modifications in intracellular calcium regulation, and the stimulation of proteolytic enzymes. The perturbation of ion transportation through the cellular membrane may result in cellular depolarization and consequent impairment of membrane integrity. The aforementioned phenomenon may lead to an increase in the entry of extracellular calcium ions, thereby exacerbating cellular dysfunction and promoting cellular demise [38].

Myocardial ischemia has an impact on intracellular calcium handling. The presence of ischemia may result in a disturbance in the regulation of calcium within the cells of the myocardium, ultimately resulting in an increase in the concentration of calcium ions within the cell. The aforementioned phenomenon has the potential to negatively impact the contractility of the myocardium. Additionally, it can facilitate the activation of multiple

proteolytic enzymes, such as phospholipases and calpains, which can exacerbate the impairment of cellular structure and function [39], [40].

Prolonged ischemia can cause a gradual deterioration in myocardial function due to the absence of oxygen and nutrients. This can ultimately lead to irreversible cellular damage and death. Cell death caused by ischemia, known as necrosis, usually initiates in the subendocardial area of the heart. This region is particularly susceptible to ischemic damage due to its high oxygen requirements and restricted collateral blood supply. In cases where the ischemic episode endures, there is a possibility for the progression of necrosis, which can affect a greater extent of the myocardium, ultimately resulting in the emergence of myocardial infarction [41].

The reinstatement of blood circulation to the ischemic heart muscle, commonly known as reperfusion, is a crucial measure in the treatment of myocardial ischemia. Reperfusion injury, a well-known phenomenon, can also be a contributing factor to myocardial injury during reperfusion [42]. Reperfusion is a process that involves the reintroduction of nutrients and oxygen to the ischemic myocardium. This process can lead to the generation of reactive oxygen species (ROS), which have the potential to cause oxidative damage to cellular components, including lipids, proteins, and DNA. Furthermore, the process of reperfusion has the potential to trigger the initiation of inflammatory cascades and the mobilization of leukocytes towards the affected myocardial tissue, thereby intensifying the extent of tissue injury [43].

The pathophysiology of ischemia encompasses a significant aspect related to the emergence of arrhythmias, which are electrical abnormalities that result from the modifications in cellular electrophysiology caused by ischemia [44], [45]. The ischemic myocardium's electrical instability can present itself in different forms of arrhythmias, which can range from premature beats that are relatively harmless to fibrillation or ventricular tachycardia that can be life-threatening.

The primary cause of electrical changes in the ischemic myocardium is the disparity of ion concentrations through the cell membrane, along with changes in the function of transporters and ion channels The build-up of extracellular potassium in ischemic events may result in a reduction of the resting membrane potential, thereby influencing the electrical stimulation of

myocardial cells and facilitating the onset of arrhythmias. Likewise, the dysfunction of intracellular calcium regulation may play a role in the development of arrhythmias by impacting the myocardium's contractile performance and refractory period.

In addition, the diverse characteristics of ischemic injury have the potential to generate areas of electrical non-uniformity in the myocardium. These regions can act as a foundation for the onset and spread of reentrant arrhythmias. Reentry is a physiological process in which electrical impulses circulate repeatedly within the cardiac tissue, resulting in the persistence of an irregular heartbeat. The formation of reentrant circuits may be facilitated by areas of unidirectional block or slow conduction in the ischemic myocardium [46].

Arrhythmias that are induced by ischemia can have noteworthy clinical implications, considering that they may impede cardiac output and worsen myocardial ischemia by augmenting myocardial oxygen demand. In instances of heightened severity, the emergence of malignant ventricular arrhythmias, e.g. fibrillation or ventricular tachycardia, may result in hemodynamic collapse and sudden cardiac fatality [47].

The pathophysiology of myocardial ischemia is a multifaceted and dynamic phenomenon that entails a complex interplay of structural, metabolic, and electrical alterations within the myocardium, as evidenced by the available literature. Myocardial ischemia is primarily caused by an inequilibrium between the supply and demand of oxygen in the myocardium, which can trigger a series of cellular responses such as disrupted ion transportation, modified calcium regulation, and the initiation of proteolytic enzyme activity. Prolonged ischemia can lead to injury, cellular dysfunction, and eventual cell death. Furthermore, the electrical fluctuation of the ischemic myocardium may contribute to the emergence of arrhythmias, which can result in noteworthy clinical implications and worsen myocardial ischemia.

1.4.3. Clinical Manifestations

Depending on factors like duration, severity, and location, myocardial ischemia can cause a wide range of different clinical manifestations. A few examples of common symptoms are:

- Chest pain due to insufficient blood supply to the heart muscle is called angina pectoris [48, p. 12], [49]. Depending on the duration, frequency, and triggers, angina can be characterized as stable, unstable, or variant [48].

- Myocardial ischemia can occur in a silent form, known as silent ischemia, and only be discovered by chance during cardiac testing [50].
- A heart attack, also known as the myocardial infarction, occurs when muscle of heart's cells die from a lack of oxygen for an extended period of time [51]. Those affected may have acute chest pain, difficulty breathing, nausea, vomiting, and profuse sweating.
- Failure of the heart to pump blood adequately is known as heart failure, and it can be the result of either persistent myocardial ischemia or myocardial infarction [52].
- Ischemic events can set off arrhythmias, or abnormal cardiac rhythms, which can have fatal implications including ventricular fibrillation or ventricular tachycardia [53].

1.5. Advanced Imaging Modalities for Myocardial Ischemia

Myocardial ischemia happens when there is a decrease in the blood supply to the heart muscle and therefore a lack of nutrients and oxygen. Ischemia must be diagnosed quickly and evaluated precisely in order to be effectively treated and managed. Recently developed imaging techniques have allowed for more precise diagnoses, more precise risk assessments, and more precise revascularization procedures. In just over a thousand words, this article discusses the most useful advanced imaging techniques for myocardial ischemia.

1.5.1. Cardiac Magnetic Resonance (CMR)

Magnetic fields and radio waves are used in cardiac magnetic resonance imaging (CMR), a noninvasive imaging method, to provide high-resolution images of the heart's function and structure [54], [55]. Myocardial ischemia can be evaluated with CMR since it measures perfusion, vitality, and contractile function of the heart.

Myocardial tissue properties can be evaluated thanks to CMR's high spatial resolution and strong soft tissue contrast. Furthermore, it does not use contrast chemicals and does not require ionizing radiation. Patients experiencing claustrophobia or those who have had metal implants are not good candidates.

1.5.2. Positron Emission Tomography (PET)

Injectable radiotracers that produce positrons are used in Positron Emission Tomography (PET), a nuclear-imaging technique. Myocardial ischemia may be evaluated with precision with PET because of the quantitative information it offers on metabolism, blood flow, and viability in the heart muscle [56].

The fundamental benefit of PET is its capacity to identify ischemia with high sensitivity and specificity, and to evaluate the severity and extent of the disease. By locating viable myocardium that could gain from revascularization, it can also guide revascularization techniques. PET is less widely available than other imaging modalities because it subjects patients to radiation that is ionizing and calls for the use of a cyclotron facility for the synthesis of radiotracers.

1.5.3. Single-Photon Emission Computed Tomography (SPECT)

Myocardial perfusion and function can also be evaluated with Single-Photon Emission Computed Tomography (SPECT), an alternate nuclear imaging technique which employs gamma-emitting radiotracers [57]. Because of its low cost and widespread availability, SPECT is often employed in the diagnosis of myocardial ischemia.

Wall motion anomalies, ejection fraction, and myocardial viability are only a few of the functional cardiac parameters that can be assessed with SPECT. It can also be used to direct revascularization decisions by pinpointing ischemic regions in need of treatment. However, SPECT patients to radiation that is ionizing and has inferior spatial resolution than PET and CMR.

1.5.4. Computed Tomography Angiography (CTA)

Noninvasively capturing high-resolution pictures of the coronary arteries, computed tomography angiography (CTA) relies on X-ray technology. Myocardial ischemia can be evaluated by measuring parameters including plaque composition and coronary artery stenosis [58], [59].

Coronary computed tomography angiography (CTA) has excellent diagnostic accuracy for diagnosing serious coronary artery disease as well as can provide useful information regarding coronary anatomy, which is essential for planning revascularization treatments.

When comparing, invasive coronary angiography (CTA) results in significantly lower radiation doses for patients. Patients with renal impairment may have issues with the application of iodinated contrast agents, that are necessary for the procedure [59].

1.5.5. Contrast Echocardiography

To better see the heart's anatomy and function, contrast echocardiography uses ultrasonography in combination with intravenous contrast chemicals. Myocardial ischemia patients benefit greatly from its use since it allows for a more accurate evaluation of myocardial perfusion and viability [60].

The benefits of contrast echocardiography are its non-invasive characteristics, extensive accessibility, and comparatively lower expenses in comparison to other sophisticated imaging techniques. Furthermore, the procedure does not subject patients to radiation that is ionizing and can be conducted either in the outpatient facility or at patient's bedside. The utilization of contrast agents facilitates enhanced demarcation of the endocardial border, superior evaluation of regional wall motion anomalies, and assessment of myocardial perfusion, thereby aiding in the identification and measurement of ischemia [61], [62].

1.6. Artificial Intelligence

The goal of artificial intelligence (AI) research is to develop computer systems with capabilities analogous to those of the human brain, including perception, language processing, decision-making, and decision-making based on incomplete or conflicting data. The performance of AI systems may be improved over time by analyzing data with statistical models and algorithms to learn.

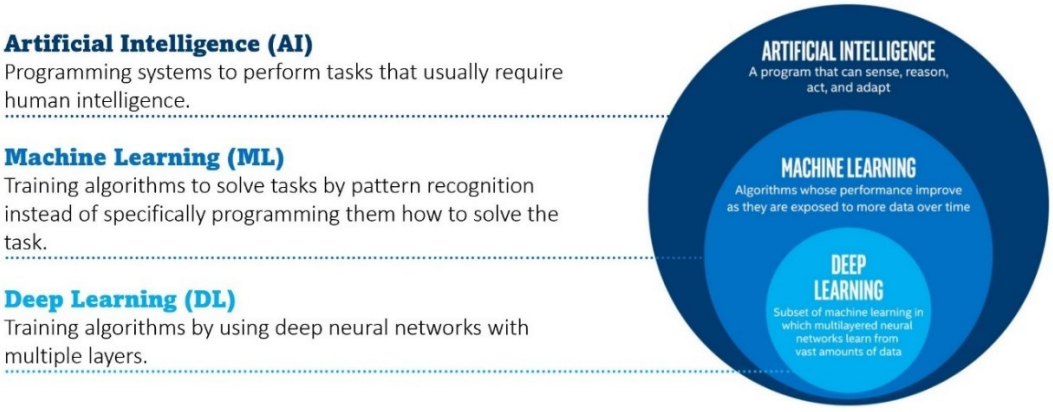

Figure 2. Artificial Intelligence and its sub-specializations.

Some examples of artificial intelligence, as shown in Figure 2, are:

1. *Rule-based systems*: Systems that rely on a set of rules established in advance to guide decision-making and behavior are called rule-based systems [63].
2. *Machine Learning*: Machine Learning (ML) refers to pre-programmed computer systems with the ability to learn new tasks automatically [64]. They utilize algorithms to sift through data in search of trends or forecasts.
3. *Deep Learning:* When it comes to analyzing data and finding patterns, deep learning is a sort of machine learning that employs artificial neural networks that mimic the function and structure of the human brain [65].
4. *Natural Language Processing*: One branch of artificial intelligence, Natural Language Processing (NLP), is devoted to just processing and comprehending human language so that computers can do the same [66].

Numerous sectors, from healthcare and banking to retail and manufacturing, can benefit from AI's many features. Numerous medical procedures, from diagnosis to treatment planning to drug development to patient monitoring, can all benefit from the usage of AI. Security and data privacy, algorithmic prejudice, and the possibility of job displacement are just a few of the ethical, legal, and societal problems brought up by the use of AI in healthcare. In spite of these obstacles, AI has great promise for enhancing healthcare delivery in many ways, including through better diagnosis and treatment, lower healthcare costs, and better patient outcomes [67].

1.6.1. AI in Medicine

The use of AI in medicine has potential to dramatically improve diagnostic precision and therapy timeliness. Images, genetic data, and Electronic Health Records (EHRs) are just a few examples of the types of medical data that may be analyzed by AI to uncover trends and predict patient outcomes [68]. The ability to detect and diagnose illnesses at an early stage is one area wherein AI has shown great promise in the medical field. AI algorithms may examine medical pictures like MRIs, X-rays, and CT scans to look for symptoms of cancer and other illnesses in their earliest stages [69]. The sooner a disease is identified and treated, the better the chances of a positive prognosis and even survival for the patient. The use of AI in tailoring care to an individual patient is another promising area of application [70]. AI systems can determine the best course of therapy for an individual patient by studying their medical records, genetic data, and other relevant data. Positive therapeutic results and fewer unwanted side effects may result from this.

AI has applications beyond just medical diagnosis and treatment, including better patient monitoring and overall care. For instance, AI systems may monitor things like a patient's vitals, medication intake, and activity levels to look for deviations that could point to a deterioration in health. By stepping in before issues arise, physicians and other medical staff can hopefully improve patient outcomes. Despite these positives, however, there are also many questions and issues that arise when AI is used in the medical field. AI algorithms' possible propensity for prejudice and inaccuracy is a major cause for worry. Incorrect or improper diagnoses or treatment suggestions might be generated by AI systems if they were trained using biased or insufficient datasets.

The prospect for AI to supplant human decision-making and clinical knowledge is another source of concern. Medical experts and other professionals will still need to play a pivotal role in patient care, even with the help of AI for diagnosis and treatment planning.

There are additional ethical and legal questions that need to be answered before AI may be used in the medical field. Concerns concerning patient security and data privacy are prompted, for instance, by the employment of artificial intelligence systems for such analysis [71]. Patient information must be protected and managed in accordance with applicable laws. Overall, AI has great potential to dramatically alter the medical industry by enhancing diagnostic precision and treatment timeliness. AI

1.6.2. Machine Learning

Machine learning (ML) is the core branch of AI concerned with development of algorithms with the ability to analyze data and draw conclusions or spot trends. To learn from experience and get better over time, ML algorithms employ statistical methods of data analysis.

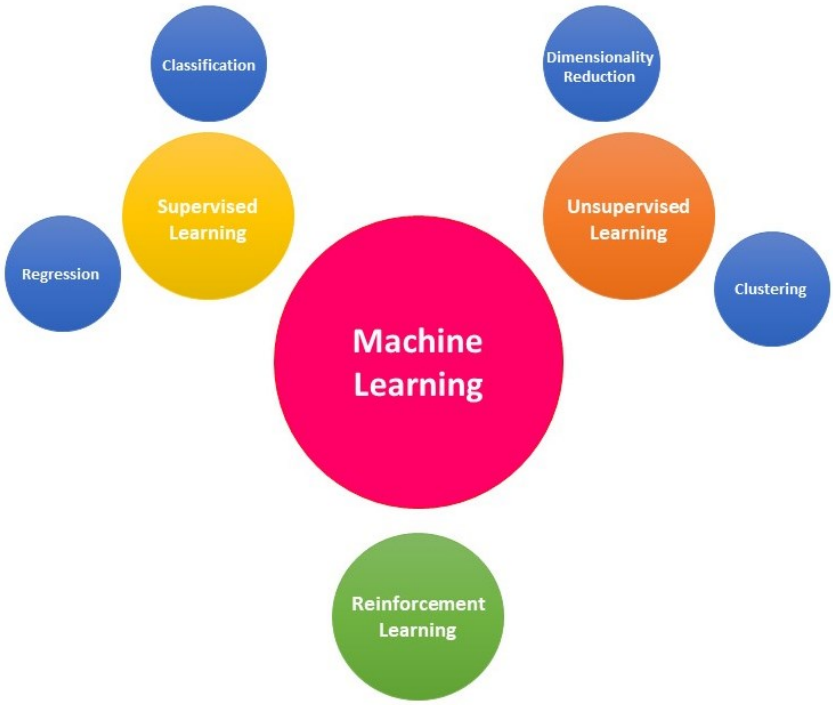

Figure 3. Categorization of machine learning.

Machine learning may be broken down into numerous subfields as shown in Figure 3:

1. *Supervised learning:* involves the utilization of a labelled dataset to train an algorithm, whereby both the input data and desired output are provided. The algorithm acquires knowledge of the correlation between the input characteristics and the outcome variable, thereby enabling it to generate forecasts for novel, unobserved data. Frequently utilized supervised learning methodologies encompass logistic regression, linear regression, decision trees and support vector machines [72].

2. *Unsupervised learning*: is a machine learning technique whereby an algorithm is trained on dataset that lacks labelling, and only input features are available for analysis. The objective of the algorithm is to identify patterns or structures inherent in the data. This mode of learning proves to be advantageous in applications such as dimensionality reduction, clustering, and anomaly detection. Unsupervised learning methods that are frequently employed include hierarchical clustering, k-means clustering, and PCA (principal component analysis) [73].

3. *Reinforcement learning:* is a type of machine learning algorithm that enables an agent to learn how to make the right choices by responding to an environment. The agent receives feedback in the form of rewards or the penalties for its actions and utilize this information to update its decision-making strategy over time. The learning agent is subject to a feedback mechanism that involves receiving either penalties or rewards for each action it undertakes. This feedback is then utilized to update the agent's knowledge and enhance its decision-making capabilities. Reinforcement learning methods have extensive applications in various domains, including robotics, control engineering, and artificial intelligence for gaming, as exemplified by AlphaGo [74], [75].

In addition to healthcare, retail, finance, and manufacturing, ML has numerous potential uses in other sectors. ML has several potential applications in the healthcare industry, including the prediction of patient outcomes, the discovery of new medication targets, and the enhancement of medical image processing [67].

Concerns about algorithmic prejudice and the possibility of employment displacement are only two examples of the ethical, legal, and societal issues brought up by ML's application. Despite these obstacles, ML has potential to revolutionize the healthcare system by increasing diagnostic precision, streamlining treatment, lowering costs, and improving patient outcomes.

1.6.3. ML in Computer-Aided Diagnosis

For many years, medical professionals have relied on computer algorithms to help them analyze medical images and make diagnoses; recently, however, machine learning (ML) has shown considerable promise in this area of computer-aided diagnosis (CAD) [76]. With the use of CAD systems, medical image analysis may be performed more precisely and rapidly, easing the burden on radiologists while also enhancing patient care. Multiple ML methods, such as supervised and unsupervised learning and even deep learning, can be applied to computer-aided design (CAD) [15]. Algorithm training on a labelled dataset where the accurate diagnoses are known beforehand is what supervised learning is all about. Data is clustered or grouped according to similarities or differences without being given the proper diagnosis in advance, as is the case with unsupervised learning [73]. One sort of neural network, known as "deep learning," excels at handling massive, intricate data sets.

Though ML's applications in CAD have shown much potential, several obstacles and restrictions must still be overcome. Training ML algorithms require huge, high-quality datasets, which presents a significant difficulty in and of itself. In the case of uncommon diseases or conditions, acquiring such data sets can be arduous and costly. Further complicating matters, ML algorithms may be biased or inaccurate. Algorithms run the risk of providing incorrect or improper diagnoses or treatment suggestions if they were trained on biased or inadequate data. To accurately diagnose a population, it is crucial that the data used for training be as diverse and representative as possible [77], [78].

By enhancing the accuracy of medical image analysis and diagnosis, machine learning has the potential to significantly impact the field of computer-aided diagnosis. Radiologists can get help from ML algorithms in spotting and categorizing anomalies, which could lead to quicker diagnosis and better care. The application of ML in CAD is fraught with difficulties

and restrictions, but the field of medical imaging stands to gain much from exploring its possibilities.

1.6.4. Deep Learning and Image Classification

Deep learning is a specialization of machine learning that makes extensive use of networked computers programmed to act as neural networks. In recent years, it has emerged as a potent resource for many fields, including computer vision, NLP, and speech recognition. The field of medical imaging has benefited greatly from deep learning in recent years, especially in the application's ability to classify images. Automated analysis of medical images for the detection of features or patterns is known as medical image classification [79]. Diseases can be diagnosed more accurately, treatment outcomes can be tracked, and surgical procedures may be planned with more precision with this information. Since deep learning can learn and adapt to new situations automatically, it has been shown to be especially useful in this domain. Among deep learning's many benefits for medical picture categorization is its speed and accuracy in handling massive datasets. Because of the prevalence of the use of huge datasets in the training of machine learning models in the medical profession, this is of paramount importance. Using their intuitive understanding of data, deep learning algorithms can swiftly modify their settings to maximize precision. Automatic feature extraction from image data is another area where deep learning excels [80]. Extracting features for use in traditional picture classification methods is a laborious and prone-to-error process. On the other hand, deep learning algorithms can be trained to discover how to independently and accurately locate important data features.

Diagnostic imaging for diseases as diverse as lung cancer, breast cancer, and Alzheimer's disease has all benefited from the application of deep learning in recent years. Using mammography scans as training data, a deep learning network was able to detect breast cancer with an accuracy of 90.5% [81]. With a sensitivity of 88.5% and a specificity of 90.1%, another study employed deep learning to classify brain MRI data as normal or abnormal automatically [82]. Deep learning has been applied to image segmentation, the process of splitting an image into segments, in addition to classification [83]. This can help in the diagnosis of malignancies and the localization of blood arteries inside medical pictures. One study even managed to achieve 95% segmentation accuracy for liver cancers in CT scans

using deep learning, proving its usefulness in this field [84]. There are certain drawbacks to using deep learning for image classification on medical image data, despite the many benefits it provides. Big labelled data sets are needed to train the algorithms, which presents a significant problem [85]. Due to ethical and privacy concerns reasons, the medical industry presents unique challenges when it comes to gathering labeled data. It's also important that deep learning models can be understood by humans. It can be difficult to decipher how a deep learning algorithm arrived at a certain conclusion, leading to the common perception that such algorithms should be avoided. Especially in the realm of medicine, where knowing the rationale behind a treatment or diagnosis suggestion is crucial, this can be a major issue.

Finally, it's clear that deep learning has emerged as a powerful resource for diagnostic image categorization. Its strengths include fast and precise data processing, the capacity to extract features automatically from image data, and a relatively small memory footprint. Despite the difficulties of applying deep learning in medicine, such as the requirement for vast volumes of labelled data and the requirement for interpretability of models, this field of study has great promise for advancing medical diagnosis and treatment.

1.6.5. Transfer Learning and Feature Extraction

Machine learning relies heavily on the integration of several key ideas, including transfer learning and feature extraction. Feature extraction is the process of choosing and extracting useful characteristics from a dataset [86], while transfer learning is the application of information gained in one domain to another [20]. This section will discuss the synergy between feature extraction and transfer learning, as well as the advantages of each and the most common approaches of implementing them.

Using what you've learnt in one context or field and applying it to another is called transfer learning. When training data is scarce for the intended job or building a model from scratch is too computationally intensive, transfer learning can be an invaluable tool in the machine learning approach [19]. By leveraging the weights and topologies of previously trained models, transfer learning can be used to boost the effectiveness of newly learned models for similar tasks [19] [20], [87].

The best features in a dataset can be isolated through a procedure known as feature extraction. The goal is to make the data lower dimensional, or simpler so that it can be more easily processed and analyzed. Image recognition, audio recognition, and NLP are just few of the many fields that can benefit from feature extraction [88], [89] [90] [91]. It shines in circumstances where dataset is huge and complicated, making it difficult to spot the most important elements.

Particularly in deep learning, the two techniques of transfer learning and feature extraction are frequently utilized simultaneously. Models trained using deep learning have multiple levels of processing power and can pick up a wide variety of features. However, training such models from scratch is likely to be time-consuming and computationally costly. Through the process of transfer learning, we can employ previously learned models to solve a fresh problem. As a result, features learned by pre-trained model for new problem can be fine-tuned via feature extraction [92].

As for feature extraction and transfer learning, there are a number of well-known methods. In order to avoid overfitting, the majority of transfer learning projects employ a fine-tuning strategy in which an already-trained model is retrained on a different dataset. The pre-trained model can also be used as a fixed feature extractor, in which case its weights are not updated during the training process, and only weights of the newly added layers are trained [93].

Common methods for extracting features include independent component analysis (ICA), principal component analysis (PCA), and the non-negative matrix factorization (NMF) [94]. PCA is a linear method that projects the data over the lower dimensional space in order to reduce the data's dimensionality. ICA is a method for decomposing multivariate signals into component non-Gaussian signals. The NMF method decomposes a matrix into a collection of basis coefficients and vectors that could be used to symbolize the information.

TL (Transfer Learning) and feature extraction have many advantages. In the first place, transfer learning helps us train models over smaller amounts of data by reusing information from larger ones. This can be especially helpful in cases when collecting huge amounts of

labeled dataset would be time-consuming or costly. Second, feature extraction can aid in reducing data dimensions, making it more manageable and amenable to analysis. In some cases, this can even improve processing speed and precision [95].

Furthermore, machine learning model generalization can be enhanced through transfer learning and feature extraction. Overfitting occurs when a model works well on training data but adversely on new and unseen data [96]. This issue can be avoided through information transfer across tasks. By decreasing data dimensions and removing unimportant characteristics that may contribute to overfitting, feature extraction can also aid to improve the generalization of models.

CNN models that have been trained on one task and are then made available for use on another task are what we call "pre-trained models". Pre-trained models are effective because of the high-powered computing resources used during training and the large datasets used to feed their hidden layers. You can find pre-trained models (also called networks) in public repositories on the internet, such as the Keras applications repository and the TensorFlow hub [97], [98]. Many ML issues, such as image recognition and audio categorization, are amenable to these networks. Models that have already been pre-trained are judged according to how well they do in ImageNet competition. To improve their image recognition performance on the ImageNet dataset, scientific teams from all over the world enter an annual competition to propose an architecture for CNN .

More than 14 million photos in over 20,000 categories make up the massive ImageNet dataset. A human annotated each image in the collection. Annotation works to assign labels to photos in order to determine what category they belong to. The goal of the ImageNet competition is to create an accurate image classification system that can be applied to this database. By the middle of 2022, top-1 accuracy for pre-trained networks on this dataset had increased to 85.7%, and top-5 accuracy had reached 97.5% (EfficientNetV2L) [99].

1.7. Proposed Approach: MS-DenseNet Model

In order to perform better on image identification tasks, the MS-DenseNet deep learning model combines the benefits of the well-liked DenseNet architecture with the Multi-Scale (MS) method. In a research MS-DenseNet: Multi-Scale Dense Networks for Resource Efficient Image Classification introduced by Hieu Le and colleagues is utilized [100].

With the feed-forward convolutional neural network design known as DenseNet, each layer is connected to every other layer. This strategy promotes feature reuse, which lowers the number of parameters the network needs and increases network efficiency. However, features scale in the input image, which might be a crucial element in image identification tasks, is not taken into consideration by the original DenseNet architecture [101].

The creators of MS-DenseNet added a multi-Scale method to the DenseNet architecture to overcome this problem . In the Multi-Scale technique, the input image is processed at many scales, enabling the network to collect features at various granularities. As a result, the network is better able to identify items in the input image that are varied sizes and forms [102].

Each DenseNet block in the MS-DenseNet architecture is made up of a number of convolutional layers, which are followed by one transition layer. In order to reduce the size of network, the transition layer compresses the channel dimension and shrinks the spatial dimensions of the feature maps. All DenseNet nodes are given an extra module developed by the authors called Multi-Scale Dense (MSD). The MSD module concatenates the outputs after processing the feature maps at various sizes, assisting the network in capturing multi-scale information [102].

The effective usage of resources is another important aspect of MS-DenseNet. Through the use of depth-wise separable convolutions, the scientists developed a novel method for lowering the number of parameters in the network [103]. By doing this, the network's performance is not sacrificed while the number of parameters is reduced. Additionally, the scientists devised a brand-new training method called progressive scaling, which entails exposing the network to images of progressively larger sizes while training it. This method enables the network to learn features at various scales [104].

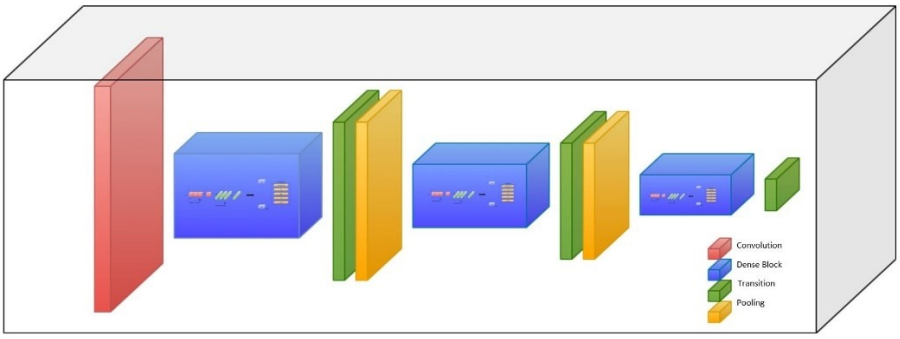

Figure 4. Proposed architecture of MS-denseNet.

In Figure 4, we used a well-known transfer learning DenseNet model as a backbone architecture of our proposed model. To reduce the size of the model, we installed three dense blocks. Inside each dense block, we replaced the regular convolution layers by Depth-wise Separable Convolution (DWSC) layers and incorporated Squeeze and Excitation (SE) module to highlight the useful feature channels while suppressing useless feature channels.

1.7.1. Depth-wise Separable Convolution

Convolutional neural networks (CNNs) have sophisticated techniques that try to minimize computational complexity while maintaining the performance of ordinary convolutions. One such technique is called depth-wise separable convolution (DWSC) [105]. Deep learning models may be trained more quickly and effectively thanks to DWSC, which is especially useful for applications like semantic segmentation, object detection, and picture recognition. Convolution is divided into two steps as shown in Figure 5: depth-wise convolution and point-wise convolution, to achieve this [106].

A collection of filters are convolved with the input feature maps in a conventional convolution to create an output feature map for each filter. The input and output channels, input spatial dimensions, and filter size all influence how computationally complicated this operation is. Large-scale model training and deployment are hampered by the growing computational burden and memory needs that come along with expanding deep learning models.

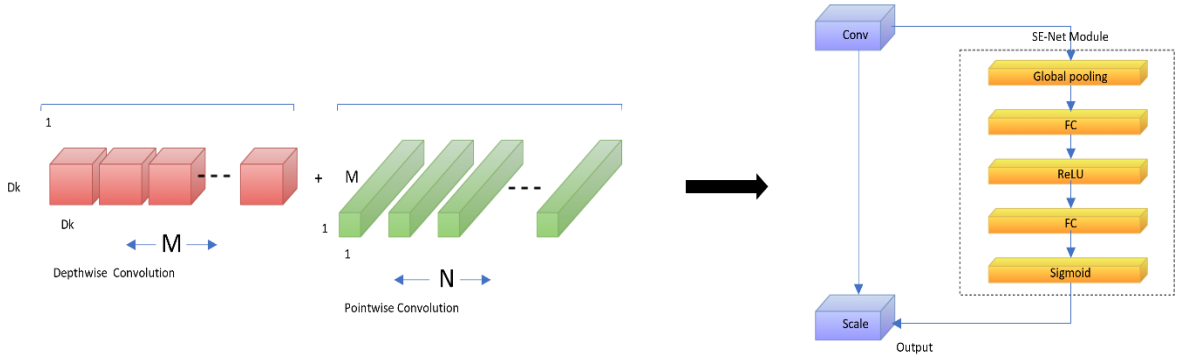

Figure 5. Depth-wise separable convolution followed by SE module inside the dense block.

By breaking down the typical convolution operation into two components, Depth-wise Separable Convolution resolves this problem:

- *Depth-wise Convolution*: This process creates just as many output channels as the input channels by applying a single filter to every input channel separately [106], [104]. As a result, the computational complexity is greatly reduced. Each filter only affects one channel. The following formula yields the depth-wise convolution:

$$Cost_{computational} = Channels_{intput} \times Size_{filter} \times Height_{intput} \times Width_{intput}$$

- Point-wise Convolution: After applying a point-wise 1x1 convolution to the output channels, the depth-wise features acquired in the previous step are combined [104], [106]. If necessary, this operation is in charge of expanding the number of output channels. The following formula yields the point-wise convolution:

$$Cost_{computational} = Channels_{intput} \times Channels_{intput} \times Height_{intput} \times Width_{intput}$$

Depth-wise Separable Convolution considerably lowers the memory requirements and computational complexity by splitting the normal convolution into these two parts. DWSC makes deep learning model deployment and training more effective by reducing the number of parameters and operations by a factor of $(Size_{filter} \times Channels_{output})$ when compared to regular convolution.

1.7.2. SE Module

The Squeeze-and-Excitation (SE) module is an architectural improvement for neural networks that aims to enhance the representational capacity of Convolutional Neural Networks (CNNs) by dynamically recalibrating feature responses on a per-channel basis. The efficacy of the "Squeeze-and-Excitation Networks" module presented by Jie Hu, Li Shen, and Gang Sun was demonstrated by its success in winning the championship for the "classification task of the ImageNet Large Scale Visual Recognition Challenge" in 2017 [107].

The SE module encompasses a pair of primary operations, namely Squeeze and Excitation. The aforementioned operations serve to capture spatial information on a global scale and recalibrate feature responses on a per-channel basis [107].

The squeeze operation is utilized to produce a channel-wise descriptor by aggregating the feature map across its spatial dimensions, namely height and width. This terminology encapsulates spatial data on a worldwide scale, condensing it into a more concise format. The process of obtaining a descriptor of size $C \times 1 \times 1$, where C denotes the number of channels in input feature map, is commonly achieved through the utilization of Global Average Pooling (GAP) [104].

The objective of the excitation operation is to re-adjust the feature responses of each channel through the acquisition of a non-linear correlation between the various channels. For this purpose, a neural network consisting of a non-linear activation function (ReLU) and two fully connected (FC) layers of small size is utilized [108]. The initial fully connected (FC) layer decreases the dimensionality of the descriptor to C/r, where r denotes the reduction ratio, commonly established at 16. Subsequently, the second FC layer restores the descriptor to its original size equals $C \times 1 \times 1$. The ultimate result is subjected to a sigmoid activation function to generate channel-specific weights within the interval of [0, 1]. These weights are subsequently applied to the initial input feature map to derive the recalibrated feature map.

The integration of the SE module into pre-existing Convolutional Neural Network (CNN) structures, such as Inception and ResNet, has yielded noteworthy enhancements in classification precision, while incurring only a slight rise in computational expenditure and model intricacy, as per the findings of researchers [104]. The SE module's principal benefit is its capacity to simulate interrelationships among channels, enabling a network to selectively accentuate or diminish particular characteristics depending on their significance for a given task.

2. AIMS AND HYPOTHESIS

In this section, we present the aims and hypothesis of our study, which focused on classifying ischemic and non-ischemic images from myocardial polar maps using the MS-denseNet model.

2.1. Aim of The Study

The primary aim of our study was to develop a robust and accurate classification model for identifying ischemic and non-ischemic images from myocardial polar maps. Ischemic heart disease is a leading cause of morbidity and mortality worldwide, and early and accurate diagnosis plays a crucial role in patient management and treatment planning. By leveraging the power of deep learning and transfer learning techniques, we aimed to develop a model that could effectively differentiate between ischemic and non-ischemic regions in myocardial polar maps.

2.2. Hypothesis

The proposed MS-denseNet model will achieve higher accuracy in classifying ischemic and non-ischemic images from myocardial polar maps compared to other transfer learning models. We hypothesize that the MS-denseNet model, with its densely connected layers and multi-scale features, will be able to capture complex patterns and features present in myocardial polar maps that are indicative of ischemia. This comprehensive feature representation, coupled with the transfer learning approach, allows the model to leverage knowledge learned from pre-training on large-scale datasets, thereby enhancing its performance in classifying ischemic and non-ischemic images.

2.3. Justification

The choice to use transfer learning and specifically the MS-denseNet model stems from its proven success in various computer vision tasks and medical imaging applications [104]. Transfer learning enables the model to leverage the knowledge acquired from pre-training on large-scale datasets, such as ImageNet, which helps in capturing generalizable features that can be applied to specific tasks [92]. Furthermore, the dense connectivity pattern in the MS-denseNet architecture facilitates feature reuse and enables effective information flow,

making it suitable for capturing intricate details in complex images like myocardial polar maps.

3. MATERIALS AND METHOD

3.1. Patients Selection

Between 2007 and 2011, a total of 138 patients with symptoms of obstructive CAD were hospitalized to Turku University Hospital, and their data is utilized in this thesis. Patients were included if they exhibited symptoms consistent with stable chest discomfort. Additionally, a prognostic for obstructive CAD was generated before testing. All patients gave their permission after being fully informed. The study obeyed the principles and rules presented in the Declaration of Helsinki and was approved by ethics board of District Hospital of Southwest Finland. Stenström's research provides further information on the patient population in the study [109].

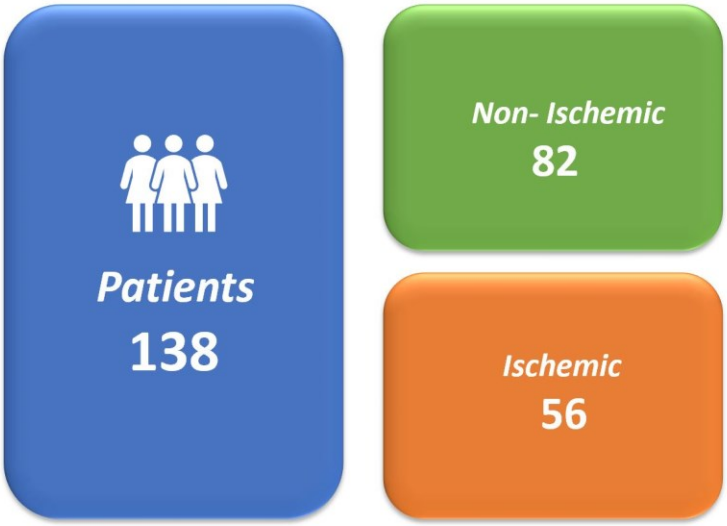

Figure 6. Patient data classified into ischemic and non-ischemic labels.

A total of 189 participants were initially enrolled, however, only 138 were ultimately included because they provided sufficient ICA and PET perfusion data in the form of stress imaging polar maps. Figure 6 presents the division of patient data into ischemic and non-ischemic labels.

3.2. Data Acquisition

For initial imaging, a Discovery VCT PET/CT scanner was employed (GE Healthcare Co., US). CT coronary angiogram (CTA) and MPI with a PET/CT hybrid were the imaging modalities of choice. A CT-based attenuation correction was performed, and then an adenosine stress perfusion PET was performed. Two minutes before the start of scan, 140 micrograms of adenosine per kilogram of body weight were administered intravenously. The patient received an intravenous bolus of oxygen-15 tagged water (900 to 1100 MBq) over the course of 15 seconds (Radiowater Generator, Hidex Oy, Finland). The heart's perfusion was then evaluated using a dynamic mode acquisition (14x5 seconds, 3x10 seconds, 3x20 seconds, and 4x30 seconds). The acquired image-based data was then reconstructed using a 2D ordered expectation-maximization method (2D-OSEM) with the following parameters: 35 cm field of view, 2 iterations, 128x128 matrix size, a 6.0 mm Gaussian post-filter, and 20 subsets.

Clinicians used invasive coronary angiography, or ICA, as part of their data collection process. For stenoses with a moderate degree (30-80%), fractional flow reserve (FFR) measurements were also performed. An expert reader used automated edge-detection software to undertake a quantitative study of ICA angiograms. Therefore, >50% ICA stenosis or FFR 0.8 was used to characterize obstructive CAD. No matter how thin the coronary artery was, if the fractional flow reserve (FFR) was more than 0.8, it was considered to be non-significant.

A single reader who was unaware of the ICA results utilized Carimas software (Turku PET Centre, Finland) to quantitatively analyze PET perfusion pictures during motion. Once the heart's orientation was determined manually, the program could easily identify the myocardium. Further, the final ROIs were fine-tuned by hand as necessary. Through mathematical modelling with a single tissue compartment model, we were able to derive quantitative polar maps of MBF values (stress) expressed in ml/g/min15. After settling on a value of 2.3 ml/g/min as the cutoff for ischemia stress MBF, we used the Rainbow colour scale to uniformly scale MBF values of stress in polar maps from 0 to 3.5 ml/g/min.

3.3. Pre-processing

A total of 138 stress MBF polar maps with accompanying ICA labels will be used in the assessment. The labels used as a benchmark will be determined by analyzing ICA data. Based on the ICA's definition of obstructive CAD, we will assign an ischemia (1) or non-ischemic (0) classification to each polar map. High-resolution 2D JPEGs of polar maps were obtained via the Carimas program. Images were first exported from Carimas at 1024 x 1024 pixels in size, before being automatically cropped and reduced in size to 256 by 256 pixels as part of the processing pipeline. All pixel values were transformed into the range [0,1]. All three of the RGB channels were used to generate the polar maps. Images of polar maps are provided as examples in Figure 7.

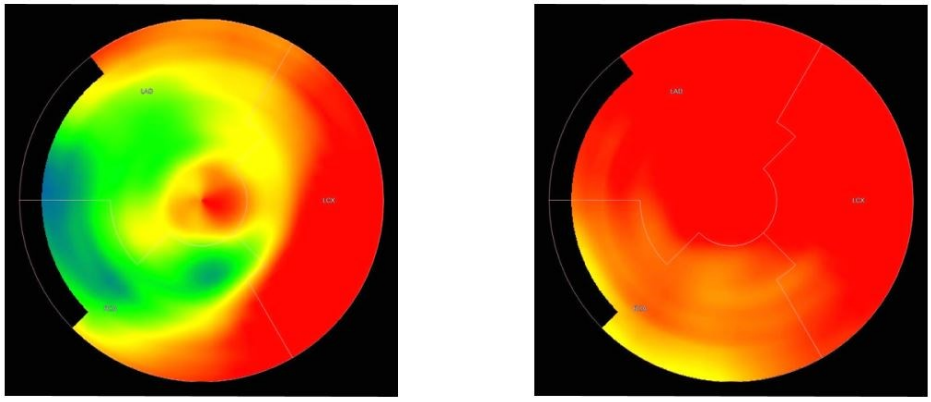

Figure 7. Non-ischemic states are depicted by the red and yellow colours. Ischemia is represented by blue and green colours.

After computer analysis, polar maps were classified as ischemia or non-ischemic. The process of labelling images is crucial to supervised learning classification problems. The ICA reference data were used to assign a value of 0 or 1 to each feature on the polar maps. A.txt file with the labels in sequential order was created.

3.4. Workflow

Here we demonstrate how transfer learning was used to categorize polar map images for signs of ischemia. In the end, a unified python code was constructed that incorporates MS-DenseNet and 12 pre-trained models, together with the necessary libraries for training and evaluating the models, after a selection of pre-trained models was chosen for this study. In

this pipeline, data was fed to the desired model for deep feature extraction. Once features were extracted, the classical ML techniques were used to identify ischemia. K-fold cross-validation was also incorporated to improve model accuracy. The code was executed, and then the outcomes were analyzed and represented graphically (Figure 8).

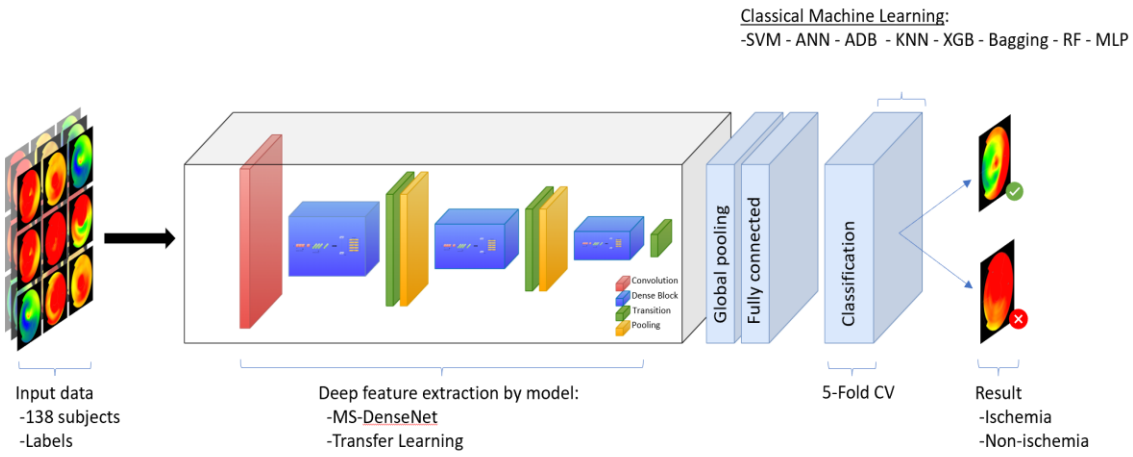

Figure 8. Classification pipeline to identify ischemia.

3.4.1. Coding

A unified code was developed to encompass all pre-trained models and their corresponding hyperparameters, in order to accommodate all 12 selected models including MS-denseNet and the need for adjustments during training. The Tensorflow library served as the primary framework for the implementation of neural network layers, architecture and hyperparameters modifications in the models. Furthermore, Keras library is employed to implement crucial configurations on pre-existing models. The environment and interpreter managers utilized in this study were Python (version 3.8) and Anaconda IDE, respectively. As per the methodology employed, the pre-existing models were retrieved from Keras repository and subsequently consolidated into a singular .Py file. The training and evaluation of models were carried out using Anaconda IDE as the Python environment manager, with the utilization of essential Python packages such as Pandas, Tensorflow, Sklearn, and Numpy. The code was developed and implemented on Kaggle community environment (online) and the Windows 10 Pro operating system.

The general framework for executing pre-trained models is outlined as follows:

a) Importing necessary libraries
b) Uploading data
c) Deep feature extraction by desired model
d) K-fold cross-validation
e) Machine learning classification
f) Evaluating performance metrics

3.4.2. Base Model

The initial stage of implementing transfer learning in any machine learning task involves the careful selection of a pre-existing model. The pre-existing Convolutional Neural Network (CNN) models must undergo training for the image classification task in this scenario. Pre-existing models designed for the purpose of image classification can be found in numerous libraries and publicly accessible websites. Keras Applications and Tensorflow Hub are widely recognized as two prominent repositories that curate a comprehensive array of pre-trained models for classification of images, which are considered to be at the forefront of the field. The present study involved the acquisition of pre-trained models from Keras repository. According to extant literature, certain models, namely VGG16, VGG19, and Inception, have been found to exhibit satisfactory performance in the context of binary classification in medical imaging tasks. Conversely, certain models have garnered comparatively less scrutiny within this field, including the DenseNet and EfficientNetB lineages. Table 2 presents a summary of the chosen pre-trained models, including their respective top-1 and top-5 accuracy scores on the source task [99].

Table 2. Selection of pre-trained models and their summary [99].

Model	***Size (MB)***	***Top-1 Accuracy***	***Top-5 Accuracy***	***Parameters***
Xception	88	79.00%	94.50%	22.9M
VGG16	528	71.30%	90.10%	138.4M
VGG19	549	71.30%	90.00%	143.7M
ResNet50	98	74.90%	92.10%	25.6M
ResNet101	171	76.40%	92.80%	44.7M

ResNet152	232	76.60%	93.10%	60.4M
InceptionV3	92	77.90%	93.70%	23.9M
InceptionResNetV2	215	80.30%	95.30%	55.9M
MobileNet	16	70.40%	89.50%	4.3M
MobileNetV2	14	71.30%	90.10%	3.5M
DenseNet121	33	75.00%	92.30%	8.1M
DenseNet169	57	76.20%	93.20%	14.3M

3.4.3. K-fold Cross Validation

The utilization of k-fold cross-validation is a prevalent resampling methodology utilized to evaluate the effectiveness and generalization capabilities of ML models in an increasingly dependable and impartial manner. The aforementioned methodology aims to mitigate the constraints associated with utilizing a solitary train-test division, which could result in an over or underestimation of veritable effectiveness of the model owing to probable partialities in the data segmentation. K-fold cross-validation involves the division of the initial dataset into 'k' partitions of equal size, with no overlap between them. The model is trained iteratively by the algorithm for 'k' iterations, where in each iteration, 'k-1' folds are utilized for training while the remaining fold is used for validation. As a result, every individual data point has the chance to be included in the validation set precisely once, thus affording a thorough assessment of the model's efficacy across diverse data subsets. In our project, the extracted features by desired model underwent 5-fold cross-validation as shown in Figure 9.

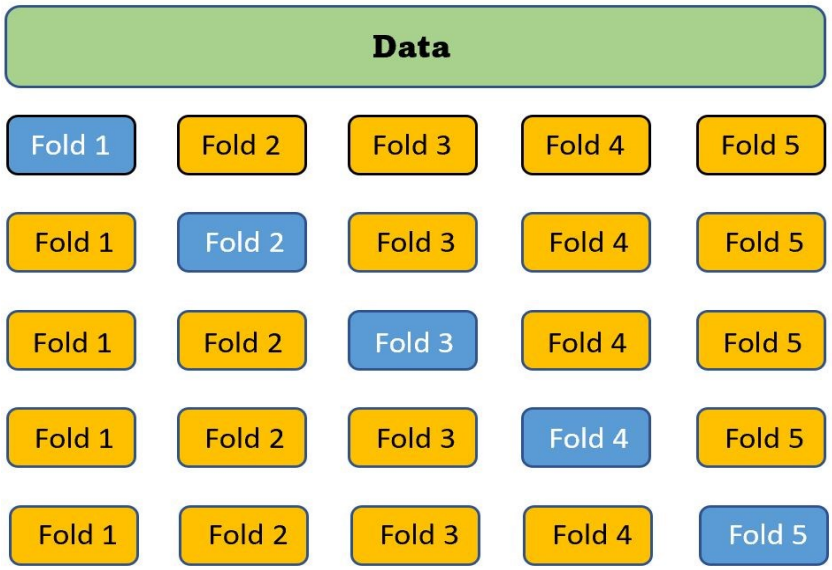

Figure 9. K-fold cross-validation, where k = 5.

The evaluation criterion, such as precision or root mean square error, is calculated for every cycle, and the ultimate evaluation is derived by taking the average of the criteria over all 'k' cycles. The aforementioned procedure serves to reduce the impact of biases resulting from data partitioning and produces a more precise and consistent evaluation of the model's authentic efficacy. The utilization of k-fold cross-validation is especially advantageous in scenarios where datasets are limited, as it optimizes the use of available data for both training and validation objectives. Nevertheless, it is worth noting that utilizing k-fold cross-validation may necessitate additional time and computational resources in comparison to a solitary train-test split, given that the model must undergo training and evaluation k times. Notwithstanding the aforementioned trade-off, k-fold cross-validation persists as a significant and indispensable methodology for evaluating the efficacy of machine learning models, aiding professionals in the processes of hyperparameter tuning, model selection, and feature selection.

3.4.4. Machine Learning Classification

The utilization of Classical Machine Learning (ML) methodologies has been extensively applied in diverse domains, which included but not limited to CV (computer vision), natural language processing (NL), speech recognition, and others. Classical machine learning (ML) has demonstrated significant achievements in various domains. However, the emergence of

deep learning, a branch of ML that employs artificial neural networks (ANN) to represent intricate data patterns, has propelled the field forward and resolved issues that were previously deemed challenging or unfeasible for classical ML methodologies. In this project, we use following classical ML techniques to identify ischemia from features extracted by desired models, as shown in Table 3:

Table 3. Classical machine learning techniques.

Abbreviation	*Algorithm*	*Technique*
SVM	Support Vector Machines	Supervised Learning
RF	Random Forest	Supervised Learning
AdaBoost	Adaptive Boosting	Supervised Learning
KNN	K-Nearest Neighbors	Supervised Learning
XGBoost	Extreme Gradient Boosting	Supervised Learning
Bagging	Bootstrap Aggregating	Ensemble Learning
MLPClassifier	Multi-layer Perceptron classifier	Supervised Learning

1. *The Support Vector Machine (SVM)* is a widely used supervised learning algorithm in the field of machine learning that is primarily utilized for addressing classification and regression problems. The Support Vector Machine (SVM) algorithm functions by identifying the most effective hyperplane that can accurately distinguish between classes through the feature space. The algorithm exhibits effectiveness in addressing spaces with a high number of dimensions and incorporates the kernel trick method to handle datasets that are not linearly separable. The utilization of diverse kernel functions e.g. polynomial, radial basis function, and sigmoid kernels, enables the linear separation of classes in higher-dimensional spaces to be more efficient. The Support Vector Machine (SVM) algorithm endeavours to optimize the margin, which is characterized as the separation between hyperplane and closest points of data from each class, known as support vectors. The optimal decision boundary, which is determined by selecting the hyperplane at maximum margin, is considered to be a crucial factor in the generalization abilities of Support Vector Machines (SVMs). The Support Vector Machine (SVM) demonstrates adaptability and efficiency in terms of

memory usage, as it solely necessitates the retention of support vectors to anticipate results [110]. The utilization of this technique has been extensively employed in various domains, such as natural language processing, computer vision, and computational biology. However, the support vector machine (SVM) algorithm exhibits certain constraints, including susceptibility to kernel choice and related parameters. Furthermore, Support Vector Machines (SVM) may demonstrate protracted training periods and restricted scalability in managing voluminous datasets. Notwithstanding these limitations, Support Vector Machine continues to be a prevalent and resilient option for numerous machine learning assignments, particularly when dealing with data of high dimensionality and intricate decision boundaries [111].

2. The *Random Forest (RF)* method is a resilient and adaptable ensemble learning approach utilized to tackle classification and regression issues within the field of machine learning [112]. The ensemble technique incorporates the forecasts of multiple base models, such as decision trees, to improve overall accuracy and reduce overfitting. The ensemble's decision trees are constructed by utilizing a random subset of training data, which is acquired via random subset of features for node splitting, and a bootstrap sampling. This approach fosters diversity among the trees. The Random Forest algorithm employs a technique of aggregating the results of individual decision trees through averaging for regression or consensus voting for classification tasks. This approach effectively mitigates the influence of individual tree biases and leads to enhanced generalization capabilities. It is widely recognized for its ability to effectively manage datasets that are of a large scale and possess numerous features. Additionally, it is known for its inherent ability to resist overfitting and its capability to rank the importance of features. Moreover, it has the capability to effectively handle imbalanced datasets and address the issue of missing data. Random Forest (RF) may exhibit limitations with respect to interpretability owing to its opaque nature, and its time of prediction may be prolonged, owing to the numerous trees utilized in the ensemble. Notwithstanding its limitations, Random Forest algorithm continues to be widely utilized and effective in addressing intricate

machine learning challenges, delivering exceptional precision and consistency across a broad range of applications [113].

3. *AdaBoost*, short for Adaptive Boosting, is an advanced ensemble learning technique utilized to tackle classification and regression problems in the context of supervised machine learning [114]. The aforementioned approach is a potent technique that functions by amalgamating the results of numerous feeble learners, usually in the form of superficial decision trees, to produce a model that is more precise and resilient. The fundamental tenet of AdaBoost entails iteratively adjusting the distribution of the training data by imparting greater weights to incorrectly classified samples. The aforementioned methodology motivates individuals with lower aptitudes to concentrate on difficult scenarios and progressively improve their abilities. Upon completion of training for each weak learner, algorithm calculates a weight for each based on its level of accuracy, whereby those with higher accuracy are assigned greater weights. In the prediction phase, AdaBoost algorithm aggregates the results of multiple weak learners by utilizing a weighted average for regression tasks or a weighted majority vote for classification tasks. The algorithm's ability to adapt and prioritize challenging instances results in enhanced generalization capabilities and decreased overfitting in comparison to individual models. AdaBoost is a machine learning algorithm that exhibits high efficacy in situations where the base learners exhibit moderate accuracy. Additionally, it has the capability to manage datasets with noise and high dimensionality. AdaBoost's performance can be affected by the presence of outliers and noisy data, as it prioritizes misclassified samples, potentially resulting in overfitting under specific conditions. Furthermore, the consecutive style of its learning procedure may lead to extended training durations in contrast to alternative ensemble techniques e.g. Random Forest. Notwithstanding these constraints, AdaBoost continues to be a widespread and resilient option for diverse machine learning implementations, providing elevated precision and performance enhancement compared to individual models [115].

4. The *k-Nearest Neighbors* (kNN) algorithm is a supervised learning technique that is commonly used in machine learning for classification and regression purposes due to its simplicity and effectiveness [116]. The k-nearest neighbours (kNN) algorithm is a type of instance-based learning approach that operates by utilizing the training data directly, without necessitating explicit training or model building. The fundamental principle of the algorithm is centred on the notion of proximity or similarity, which is evaluated through distance metrics e.g. Manhattan, Euclidean, or Minkowski distance to quantify the association between instances [117]. In the process of predicting the label or value for a novel data point, the k-Nearest Neighbors (kNN) algorithm selects the k most similar neighbours from training data and computes the output based on their corresponding labels or values. In classification tasks, the k-Nearest Neighbors (kNN) algorithm determines class labels by conducting a majority vote across the nearest neighbours [116]. Conversely, in regression tasks, the algorithm estimates the output value by computing the average of the values of the neighbouring data points. The selection of the parameter 'k' has a substantial impact on the algorithm's performance. Choosing smaller values may result in overfitting, while larger values may lead to underfitting. The k-Nearest Neighbor (kNN) algorithm is deemed suitable for addressing multi-class classification problems and can perform efficiently in spaces with high dimensions, given that a suitable distance metric is utilized. Although kNN is a straightforward algorithm, it presents certain drawbacks in relation to memory utilization and computational efficiency when handling extensive datasets. This is due to the requirement of storing the complete training dataset and calculating distances between every pair of instances. Despite its limitations, the k-Nearest Neighbors algorithm continues to be a favoured option for a range of machine learning applications, particularly in cases where the importance of interpretability, ease of implementation, and simplicity is emphasized [118].

5. *XGBoost*, also known as Extreme Gradient Boosting, is a proficient and sophisticated implementation of the gradient boosting algorithm utilized for tackling regression and classification tasks in supervised machine learning [119]. The XGBoost algorithm functions by sequentially training a series of weak learners, which are commonly

decision trees, on residual errors of previous learners in the sequence. The goal is to minimize a loss function that is differentiable. The loss function of the algorithm includes regularization terms that penalize the complexity of the model and assist in managing overfitting, leading to enhanced generalization abilities. XGBoost presents various benefits, including its capability to manage sparse data, mixed feature types, and missing values [120]. Additionally, it offers a mechanism for constructing trees in parallel, which facilitates the handling of datasets on a large scale and expedites the training process. The efficacy of the algorithm in various applications is enhanced by its ability to estimate the optimal tree depth automatically, as well as its incorporation of early stopping and cross-validation. XGBoost, akin to other boosting algorithms, exhibits sensitivity towards noisy data and is susceptible to overfitting when there are outliers. Moreover, the opaqueness of its black-box structure may constrain the interpretability in contrast to less complex models. Notwithstanding its constraints, XGBoost continues to be a prevalent option for diverse machine learning undertakings, due to its elevated precision, scalability, and adaptability, rendering it a potent instrument for addressing intricate predicaments and attaining cutting-edge performance across multiple fields [118].

6. *Bagging* (short for Bootstrap Aggregating) is a widely used ensemble learning method employed to tackle supervised machine learning tasks related to classification and regression [121]. The utilization of several base models, typically decision trees, to improve overall performance and reduce overfitting is a characteristic of the ensemble method. By collecting random samples from original training dataset with replacement, as is done in bootstrap sampling, bagging can generate numerous training sets. The distinct bootstrap samples are utilized to train each base model, which enhances model diversity and diminishes model variance. Through averaging for regression tasks or majority voting for classification tasks, bagging aggregates the results of individual base models in the prediction phase. The process of aggregation enables the ensemble to leverage the collective intelligence of a group, thereby decreasing partiality and fluctuation, and ultimately attaining enhanced generalization abilities. The utilization of bagging is especially beneficial when

confronted alongside unstable base models which exhibit a tendency to overfit since the process of aggregation has a tendency to mitigate the idiosyncratic fluctuations of individual models. The ensemble nature of bagging may present constraints in terms of interpretability, and its performance may be subject to sensitivity based on the selection of base models. Furthermore, it is worth noting that the efficacy of bagging in mitigating bias may be comparatively lower than that of other ensemble methods, such as boosting. Despite the limitations associated with bagging, it continues to be a prevalent and potent approach for addressing intricate machine-learning challenges. It offers improved stability and precision across a range of applications [10], [73].

7. The *Multilayer Perceptron* (MLP) is a type of the feedforward artificial neural network (ANN) that is commonly employed in supervised learning to address classification and regression challenges within the domain of machine learning [122]. A Multi-Layer Perceptron (MLP) is composed of an initial layer for input, one or more intermediate layers that are hidden, and a final output layer. Each of these layers is comprised of numerous interconnected nodes or neurons. The synaptic connections among neurons are distinguished by weights that undergo modification during the training phase to reduce the discrepancy between anticipated and desired outputs. In neural networks, the activation function is typically a non-linear function, such as sigmoid or the Rectified Linear Unit (ReLU). The activation function is fitted to weighted sum of inputs for every neuron, resulting in the production of its output. The process of training a Multi-Layer Perceptron (MLP) typically involves the utilization of backpropagation, which involves the computation of loss function gradient with respect to each weight through the iterative application of the chain rule. This process entails the iterative adjustment of weights to minimize the loss. The optimization procedure involves the utilization of algorithms, e.g. stochastic gradient descent or the variations of it, to modify the weights by taking into account the computed gradients [123]. Multilayer Perceptron (MLP) has the ability to represent intricate and nonlinear associations within datasets, and its efficacy can be augmented by incorporating supplementary neurons and hidden layers. Multilayer Perceptrons (MLPs) may present certain constraints, such as vulnerability to local minima through

the optimization process, complexities in identifying the most suitable architecture, and obstacles in comprehending the acquired model. Despite the aforementioned limitations, Multilayer Perceptrons continue to be a popular option for various machine learning tasks, especially in the domains of predictive modelling and pattern recognition. This is due to their ability to effectively model complex relationships within datasets that have a high number of dimensions [73].

4. RESULTS

This chapter presents the outcomes of all conducted experiments. In order to fulfil the research goals of this thesis, the outcomes of the experiments are presented in three distinct sections. Initially, the presentation and comparison of performance metrics from all pre-existing models are provided. Subsequently, following the introduction of optimal pre-trained models, the efficacy of transfer learning is evaluated through a comparison between pre-trained models and a customized convolutional neural network. Finally, a comparison was made between the most effective pre-trained models and the proposed MS-DenseNet model by analyzing their performance metrics.

4.1. Transfer Learning Analysis

With feature extraction using VGG16, the Random Forest model achieves the highest accuracy at 0.833, followed by XGBoost at 0.812 and AdaBoost at 0.811, as shown in Figure 10 and Table 4. The same ranking can be observed for Kappa and Precision metrics, with Random Forest and XGBoost consistently performing better than the other models. For F1 score and Recall, XGBoost has the highest values, followed by AdaBoost and SVM.

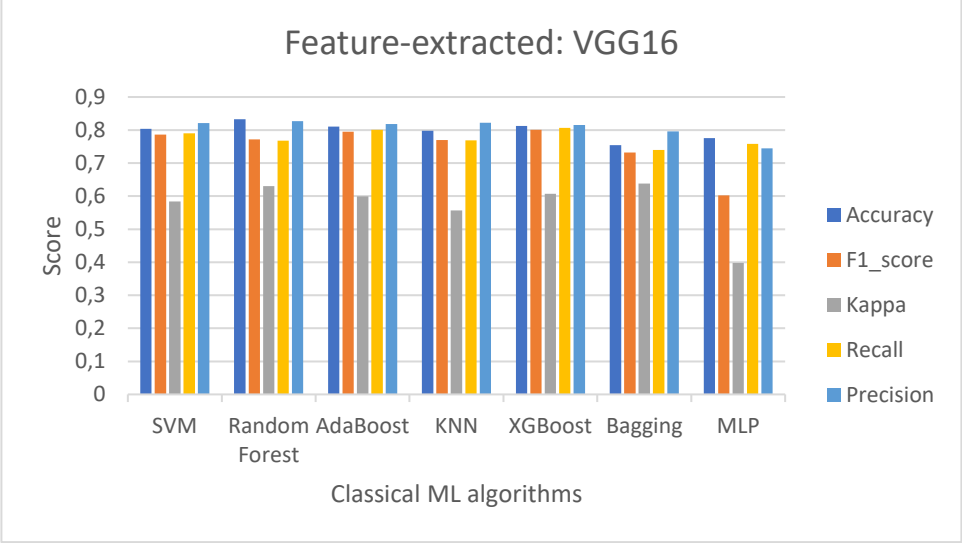

Figure 10. Summary of Evaluation Metrics for Method VGG16 with Different Machine Learning Methods. In this figure, each color represents a different evaluation metric. The VGG16 method was combined with various machine learning methods, and the corresponding evaluation metrics were measured and plotted. The legend provides a clear understanding of the color-coding used throughout the figure, enabling easy interpretation of the results.

Table 4. Comparative analysis of VGG16 when combined with various machine learning models using multiple evaluation metrics. This table presents the performance evaluation metrics for various machine learning models. Each row corresponds to a specific model, and the respective columns display the corresponding metrics. The evaluation metrics provide insights into the models' performance in terms of accuracy, precision, recall, F1 score, and Kappa coefficient. These metrics serve as indicators to assess the effectiveness and reliability of the models for classification tasks.

Model	***Accuracy [%]***	***F1_score [%]***	***Kappa [%]***	***Recall [%]***	***Precision [%]***
SVM	80.4	78.6	58.4	79.0	82.1
Random Forest	83.3	77.2	63.0	76.8	82.7
AdaBoost	81.1	79.5	59.9	80.1	81.8
KNN	79.8	77.0	55.7	76.9	82.2
XGBoost	81.2	80.1	60.7	80.7	81.5
Bagging	75.4	73.2	63.8	74.0	79.6
MLP	77.6	60.2	39.8	75.8	74.5

With feature extraction using VGG19, the AdaBoost model achieves the highest accuracy at 0.862, followed by XGBoost at 0.834 and SVM/Random Forest/KNN, all with an accuracy of 0.826, as shown in Figure 11 and Table 5. The same ranking can be observed for F1 score, Kappa, Recall, and Precision metrics, with AdaBoost and XGBoost consistently performing better than the other models.

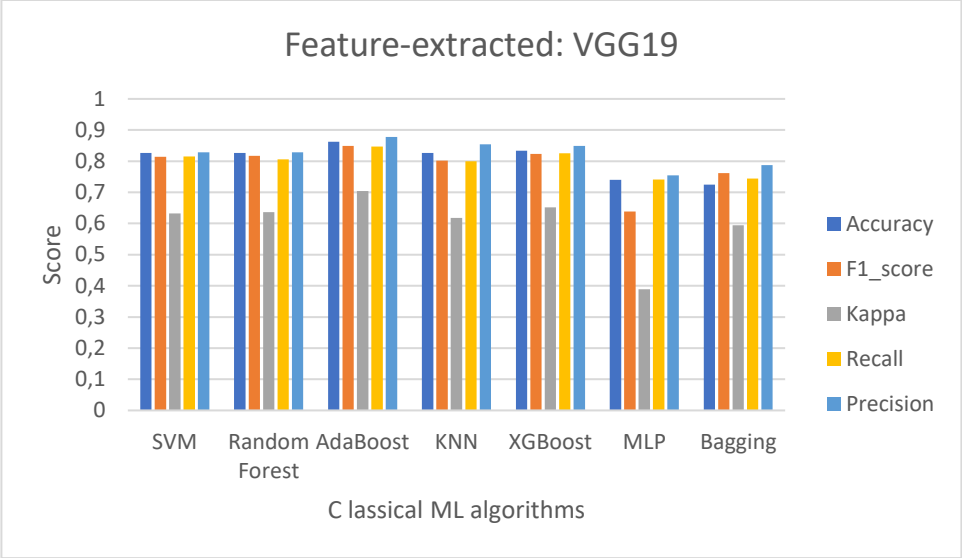

Figure 11. Summary of evaluation metrics of VGG19. See Figure 10 for the explanation of colors and symbols used in this figure.

Table 5. Evaluation metrics of VGG19. See Table 4 for the explanation of metrics used in this table.

Model	***Accuracy [%]***	***F1_score [%]***	***Kappa [%]***	***Recall [%]***	***Precision [%]***
SVM	82.6	81.4	63.2	81.5	82.9
Random Forest	82.6	81.7	63.6	80.6	82.9
AdaBoost	86.2	84.9	70.4	84.7	87.8
KNN	82.6	80.2	61.8	80.0	85.4
XGBoost	83.4	82.3	65.2	82.5	84.9
MLP	74.0	63.8	38.9	74.1	75.5
Bagging	72.5	76.2	59.4	74.4	78.7

With feature extraction using ResNet101, the SVM model achieves the highest accuracy at 0.854, followed by XGBoost at 0.847 and Bagging at 0.83, as shown in Figure 12 and Table 6. The same ranking can be observed for F1 score and Kappa metrics, with SVM and XGBoost consistently performing better than the other models. For Recall and Precision, SVM and XGBoost have the highest values, followed by Random Forest and MLP.

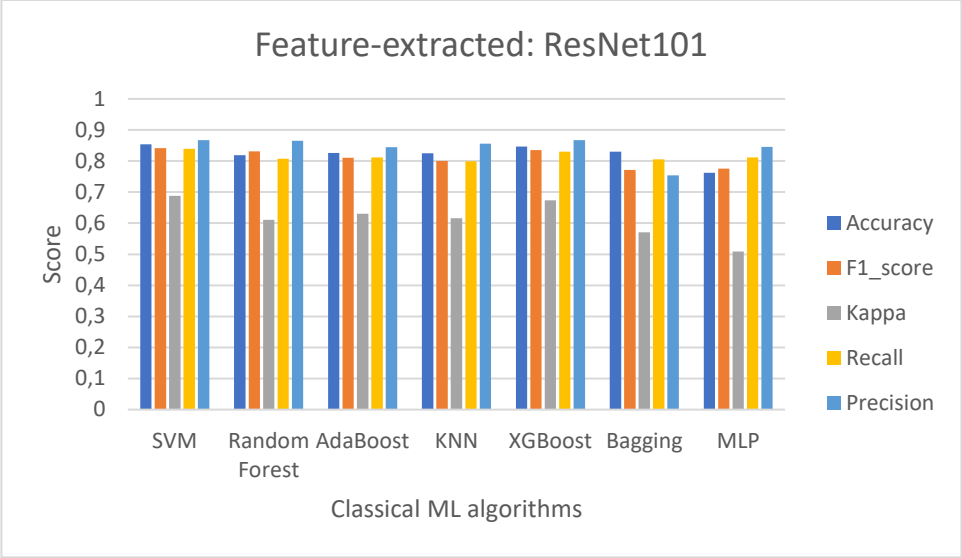

Figure 12. Evaluation metrics of ResNet101. See Figure 10 for the explanation of colors and symbols used in this figure.

Table 6. Evaluation metrics of ResNet101. See Table 4 for the explanation of metrics used in this table.

Model	***Accuracy [%]***	***F1_score [%]***	***Kappa [%]***	***Recall [%]***	***Precision [%]***
SVM	85.4	84.2	68.8	83.9	86.7
Random Forest	81.9	83.1	61.1	80.8	86.5
AdaBoost	82.6	81.1	63.0	81.2	84.5
KNN	82.5	80.0	61.6	79.9	85.6
XGBoost	84.7	83.5	67.4	83.0	86.7
Bagging	83.0	77.1	57.1	80.5	75.4
MLP	76.2	77.6	50.9	81.2	84.6

With feature extraction using ResNet50, the XGBoost model achieves the highest accuracy at 0.826, followed by AdaBoost at 0.819 and KNN at 0.818, shown in Figure 13 and Table 7. The same ranking can be observed for F1 score and Kappa metrics, with XGBoost consistently performing better than the other models. For Recall, Random Forest has the highest value, followed by XGBoost and AdaBoost. For Precision, Random Forest and KNN have the highest values, followed by XGBoost.

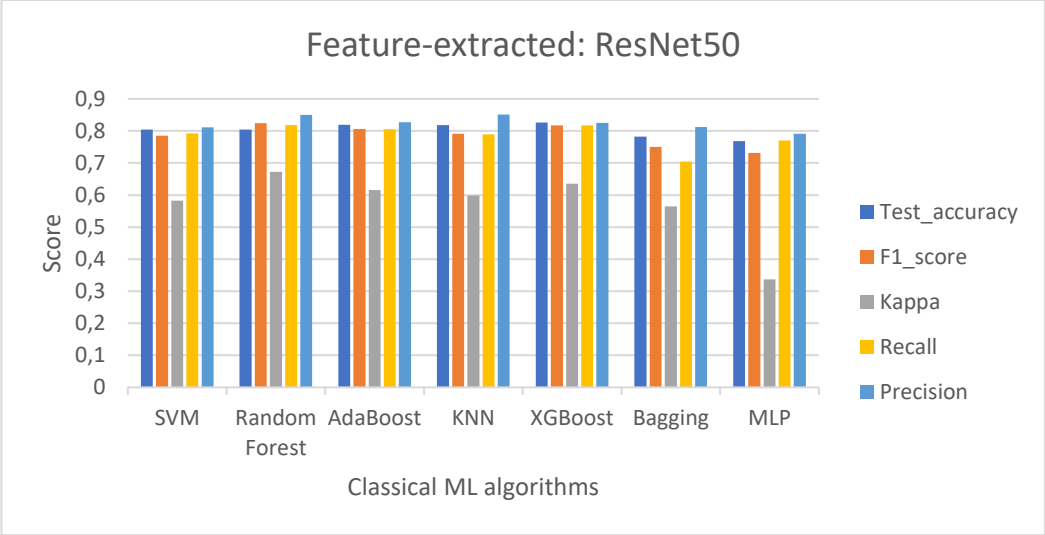

Figure 13. Evaluation metrics of ResNet50. See Figure 10 for the explanation of colors and symbols used in this figure.

Table 7. Evaluation metrics of ResNet50. See Table 4 for the explanation of metrics used in this table.

Model	***Accuracy [%]***	***F1_score [%]***	***Kappa [%]***	***Recall [%]***	***Precision [%]***
SVM	80.4	78.5	58.3	79.2	81.1
Random Forest	80.4	82.4	67.2	81.8	85.0
AdaBoost	81.9	80.6	61.6	80.5	82.7
KNN	81.8	79.1	59.9	78.9	85.1
XGBoost	82.6	81.7	63.6	81.7	82.5
Bagging	78.2	75.0	56.5	70.4	81.2
MLP	76.8	73.1	33.7	77.0	79.1

With feature extraction using MobileNetV2, the Random Forest model achieves the highest accuracy at 0.855, followed by XGBoost at 0.826 and Bagging at 0.812, as shown in Figure 14 and Table 8. The same ranking can be observed for F1 score, Kappa, Recall, and Precision metrics, with Random Forest and XGBoost consistently performing better than the other models.

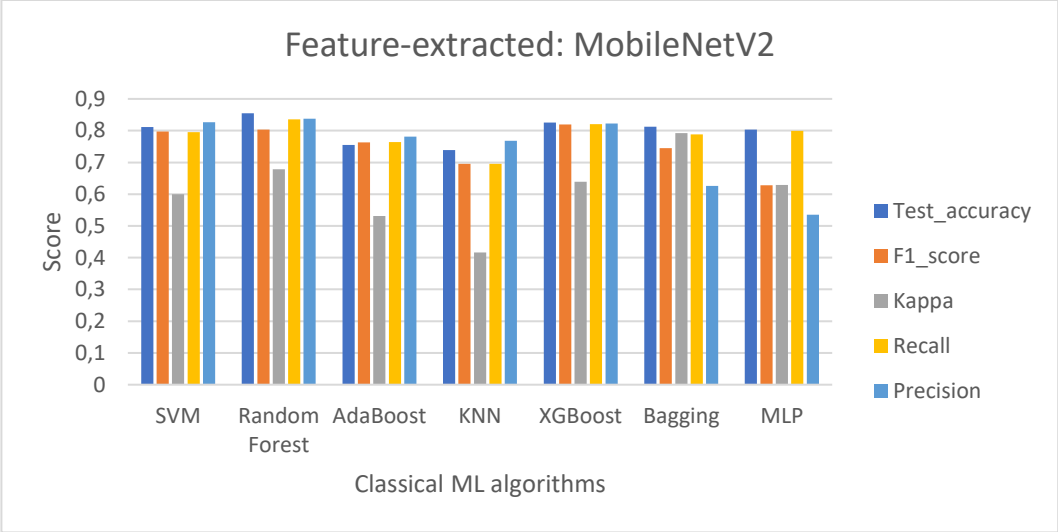

Figure 14. Evaluation metrics of MobileNetV2. See Figure 10 for the explanation of colors and symbols used in this figure.

Table 8. Evaluation metrics of MobileNetV2. See Table 4 for the explanation of metrics used in this table.

Model	***Accuracy [%]***	***F1_score [%]***	***Kappa [%]***	***Recall [%]***	***Precision [%]***
SVM	81.1	79.7	60.0	79.5	82.7
Random Forest	85.5	80.3	67.8	83.6	83.8
AdaBoost	75.5	76.3	53.1	76.4	78.1
KNN	73.9	69.6	41.6	69.6	76.8
XGBoost	82.6	81.9	63.9	82.0	82.2
Bagging	81.2	74.5	79.2	78.8	62.6
MLP	80.3	62.8	62.9	79.9	53.5

With feature extraction using MobileNet, the Random Forest and XGBoost models achieve the highest accuracy at 0.877, as shown in Figure 15 and Table 9. XGBoost has the highest F1 score at 0.869, followed by AdaBoost at 0.839 and Random Forest at 0.838. For Kappa, XGBoost and Random Forest perform better than the other models. For Recall, XGBoost has the highest value, followed by Random Forest and Bagging. For Precision, XGBoost has the highest value, followed by KNN and AdaBoost.

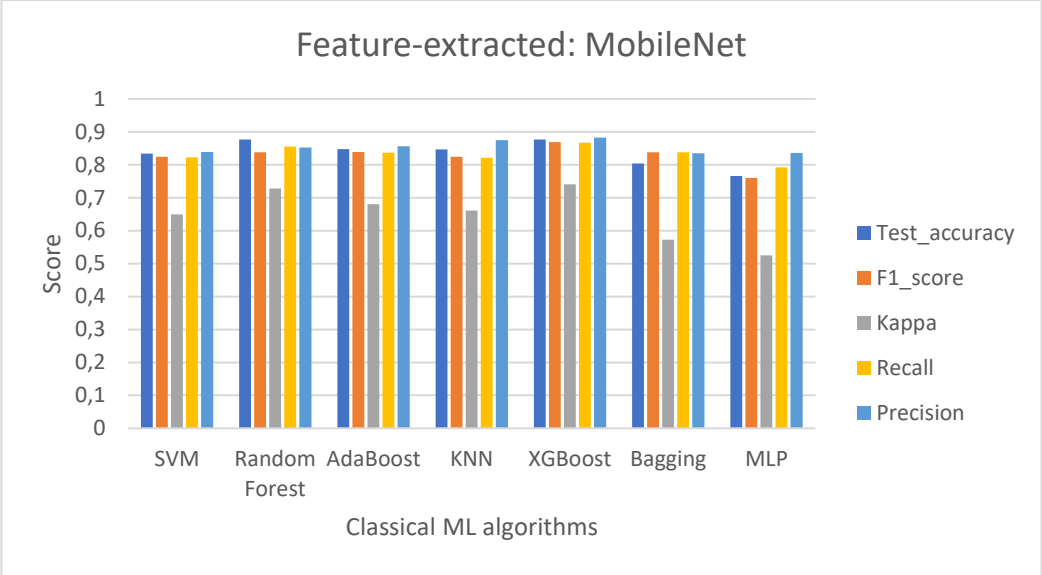

Figure 15. Evaluation metrics of MobileNet. See Figure 10 for the explanation of colors and symbols used in this figure.

Table 9. Evaluation metrics of MobileNet. See Table 4 for the explanation of metrics used in this table.

Model	***Accuracy [%]***	***F1_score [%]***	***Kappa [%]***	***Recall [%]***	***Precision [%]***
SVM	83.4	82.4	64.9	82.2	83.9
Random Forest	87.7	83.8	72.8	85.5	85.2
AdaBoost	84.8	83.9	68.0	83.7	85.6
KNN	84.7	82.4	66.1	82.1	87.5
XGBoost	87.7	86.9	74.1	86.7	88.3
Bagging	80.4	83.8	57.3	83.8	83.5
MLP	76.6	76.0	52.5	79.2	83.6

With feature extraction using InceptionResNetV2, the Random Forest model achieves the highest accuracy at 0.834, followed by XGBoost at 0.833 and SVM at 0.819, as shown in Figure 16 and Table 10. The same ranking can be observed for F1 score and Kappa metrics, with Random Forest and XGBoost consistently performing better than the other models. For Recall, SVM has the highest value, followed by AdaBoost and Random Forest. For Precision, KNN and Random Forest have the highest values, followed by XGBoost.

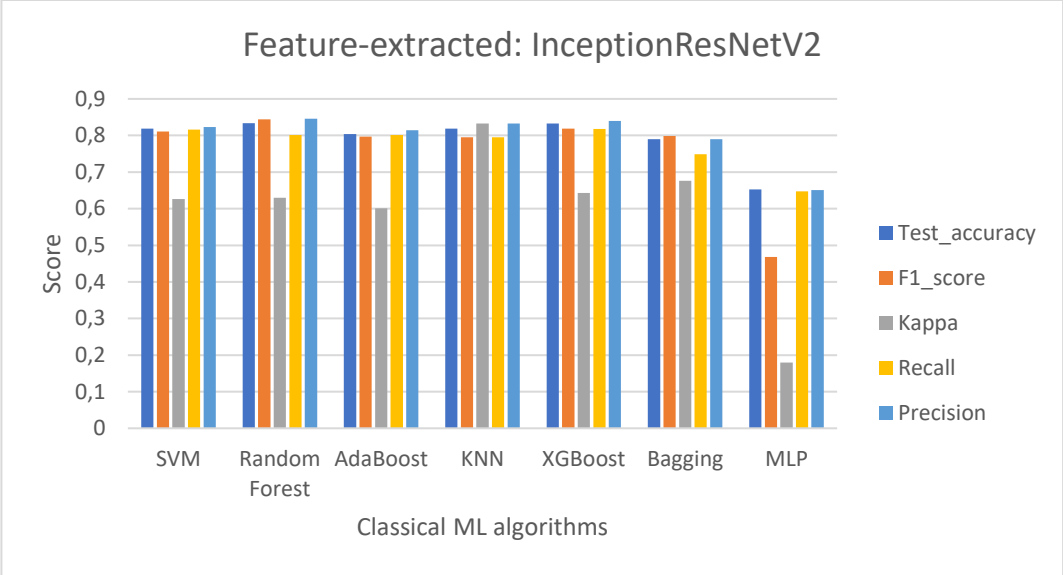

Figure 16. Evaluation metrics of InceptionResNetV2. See Figure 10 for the explanation of colors and symbols used in this figure.

Table 10. Evaluation metrics of InceptionResNetV2. See Table 4 for the explanation of metrics used in this table.

Model	***Accuracy [%]***	***F1_score [%]***	***Kappa [%]***	***Recall [%]***	***Precision [%]***
SVM	81.9	81.1	62.6	81.6	82.3
Random Forest	83.4	84.4	63.0	80.1	84.6
AdaBoost	80.4	79.7	60.1	80.1	81.4
KNN	81.9	79.5	83.3	79.5	83.3
XGBoost	83.3	81.9	64.3	81.8	84.0
Bagging	79.0	79.9	67.6	74.9	79.0
MLP	65.3	46.8	18.0	64.7	65.1

With feature extraction using InceptionV3, the XGBoost model achieves the highest accuracy at 0.79, followed by Random Forest at 0.775 and KNN at 0.767, as shown in Figure 17 and Table 11. The same ranking can be observed for F1 score and Kappa metrics, with XGBoost and Random Forest consistently performing better than the other models. For Recall, XGBoost has the highest value, followed by Random Forest and AdaBoost. For Precision, XGBoost and Bagging have the highest values, followed by Random Forest.

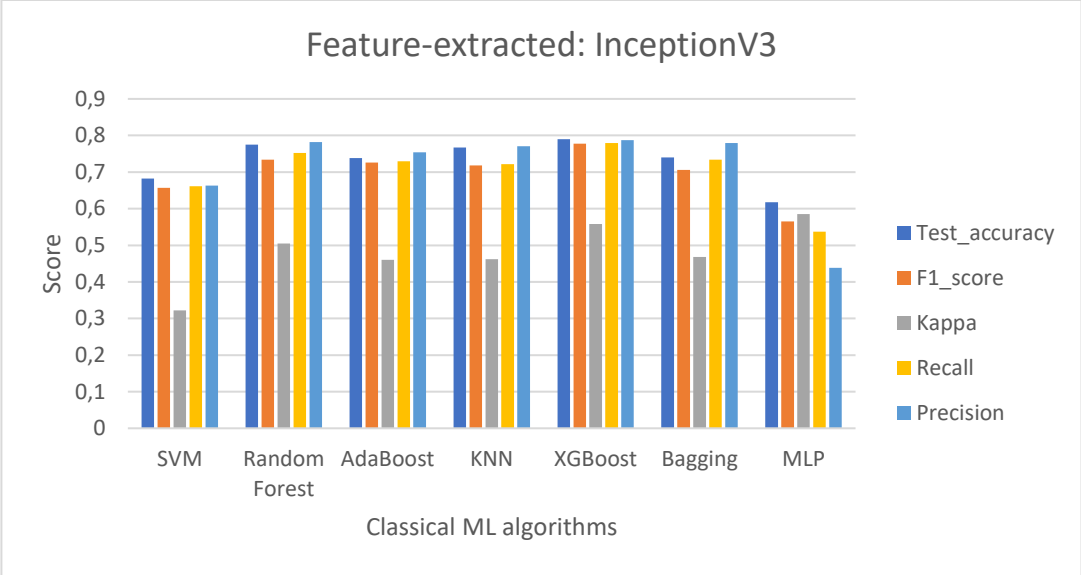

Figure 17. Evaluation metrics of InceptionV3. See Figure 10 for the explanation of colors and symbols used in this figure.

Table 11. Evaluation metrics of InceptionV3. See Table 4 for the explanation of metrics used in this table.

Model	***Accuracy [%]***	***F1_score [%]***	***Kappa [%]***	***Recall [%]***	***Precision [%]***
SVM	68.2	65.7	32.2	66.1	66.3
Random Forest	77.5	73.4	50.5	75.2	78.2
AdaBoost	73.8	72.6	46.0	73.0	75.4
KNN	76.7	71.8	46.2	72.2	77.1
XGBoost	79.0	77.8	55.8	77.9	78.7
Bagging	74.0	70.6	46.8	73.4	77.9
MLP	61.8	56.5	58.5	53.7	43.8

With feature extraction using DenseNet169, the Random Forest model achieves the highest accuracy at 0.855, followed by KNN at 0.848 and XGBoost at 0.834, as shown in Figure 18 and Table 12. The same ranking can be observed for F1 score and Kappa metrics, with Random Forest and KNN consistently performing better than the other models. For Recall, Bagging has the highest value, followed by Random Forest and AdaBoost. For Precision, KNN has the highest value, followed by Random Forest and Bagging.

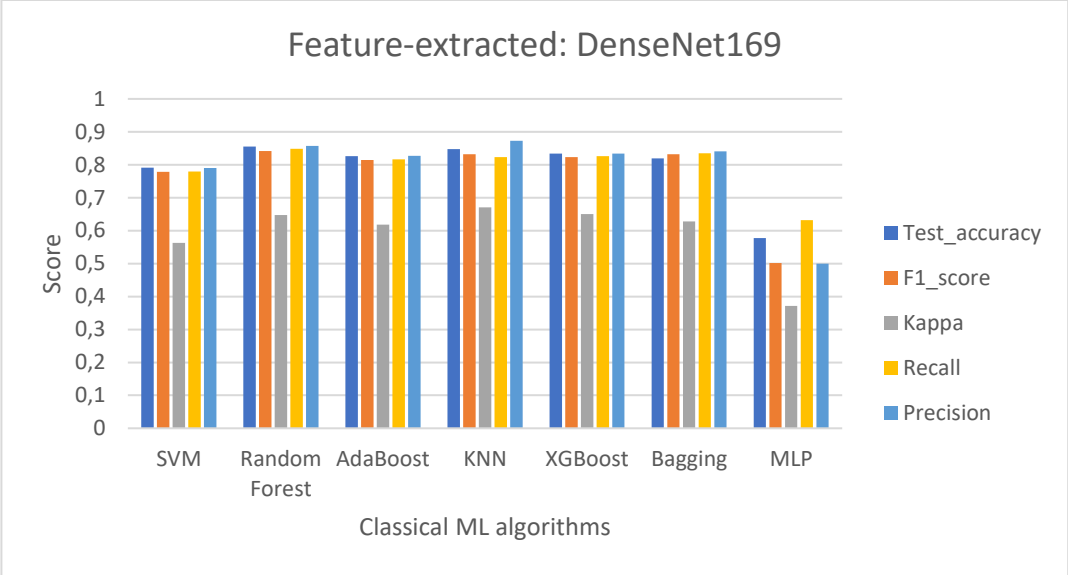

Figure 18. Evaluation metrics of DenseNet169. See Figure 10 for the explanation of colors and symbols used in this figure.

Table 12. Evaluation metrics of DenseNet169. See Table 4 for the explanation of metrics used in this table.

Model	***Accuracy [%]***	***F1_score [%]***	***Kappa [%]***	***Recall [%]***	***Precision [%]***
SVM	79.1	77.9	56.3	78.0	79.0
Random Forest	85.5	84.2	64.7	84.9	85.7
AdaBoost	82.6	81.5	61.8	81.6	82.7
KNN	84.8	83.2	67.1	82.3	87.3
XGBoost	83.4	82.3	65.0	82.6	83.4
Bagging	81.9	83.2	62.8	83.5	84.1
MLP	57.7	50.2	37.2	63.2	50.0

With feature extraction using DenseNet121, the K-Nearest Neighbors (KNN) model achieves the highest accuracy at 0.863, followed by Random Forest at 0.848 and AdaBoost and XGBoost both at 0.826, as shown in Figure 19 and Table 13Table 13. Evaluation metrics of DenseNet121.. For F1 score, Random Forest has the highest value, followed by KNN and XGBoost. For Kappa, KNN has the highest value, followed by Random Forest and AdaBoost. For Recall, Bagging has the highest value, followed by KNN and Random Forest. For Precision, KNN has the highest value, followed by Random Forest and XGBoost.

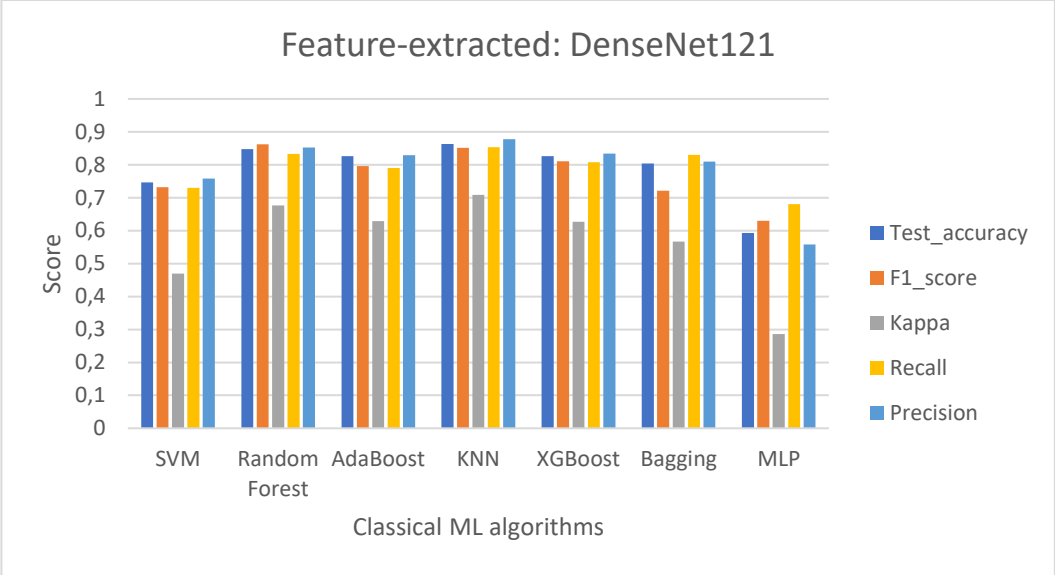

Figure 19. Evaluation metrics of DenseNet121. See Figure 10 for the explanation of colors and symbols used in this figure.

Table 13. Evaluation metrics of DenseNet121. See Table 4 for the explanation of metrics used in this table.

Model	***Accuracy [%]***	***F1_score [%]***	***Kappa [%]***	***Recall [%]***	***Precision [%]***
SVM	74.7	73.2	47.0	73.0	75.8
Random Forest	84.8	86.2	67.7	83.3	85.2
AdaBoost	82.6	79.6	62.9	79.0	82.9
KNN	86.3	85.1	70.9	85.3	87.8
XGBoost	82.6	81.1	62.7	80.8	83.4
Bagging	80.4	72.1	56.7	83.0	81.0
MLP	59.3	63.0	28.6	68.0	55.8

With feature extraction using Xception, the Random Forest model achieves the highest accuracy at 0.797, followed by XGBoost at 0.79 and Bagging at 0.775, as shown in Figure 20 and Table 14. For F1 score, Random Forest has the highest value, followed by XGBoost and AdaBoost. For Kappa, Random Forest has the highest value, followed by XGBoost and Bagging. For Recall, Bagging has the highest value, followed by XGBoost and Random Forest. For Precision, Bagging has the highest value, followed by Random Forest and KNN.

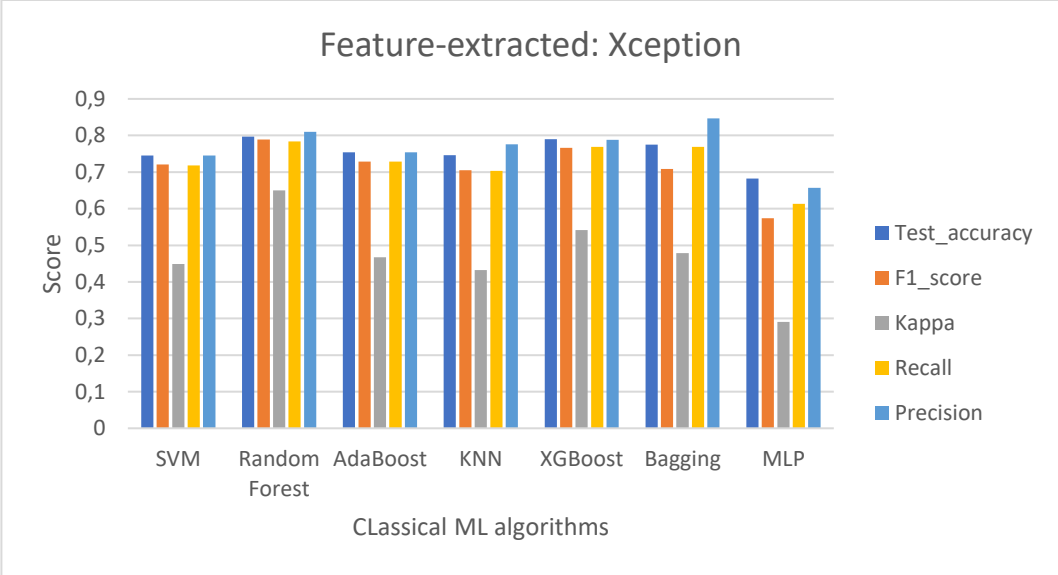

Figure 20. Evaluation metrics of Xception. See Figure 10 for the explanation of colors and symbols used in this figure.

Table 14. Evaluation metrics of Xception. See Table 4 for the explanation of metrics used in this table.

Model	***Accuracy [%]***	***F1_score [%]***	***Kappa [%]***	***Recall [%]***	***Precision [%]***
SVM	74.5	72.1	44.9	71.8	74.5
Random Forest	79.7	78.9	65.0	78.4	81.0
AdaBoost	75.4	72.9	46.7	72.9	75.4
KNN	74.6	70.5	43.2	70.3	77.6
XGBoost	79.0	76.6	54.2	76.9	78.8
Bagging	77.5	70.9	47.9	76.9	84.7
MLP	68.2	57.4	29.1	61.3	65.7

In summary, MobileNet with Random Forest and XGBoost achieve the highest accuracy among the deep feature extraction models. DenseNet121 with KNN and VGG19 with Random AdaBoost also demonstrate strong performance. The other neural networks have relatively lower performance, with InceptionV3 and Xception being the lowest performers.

4.2. Transfer Learning vs Custom CNN

Based on the experimental results, the accuracy achieved by the top 3 deep feature extraction networks (VGG19, MobileNet, and DenseNet121) ranged from 0.862 to 0.877. On the other hand, the custom CNN achieved an accuracy of 0.83 [24], which is lower than all top 3,

VGG19, MobileNet, and DenseNet121 deep feature extraction networks. Interestingly, the clinical interpretation achieved the highest accuracy of 0.87 [24], which is higher than all the deep feature extraction models except for the MobileNet model with XGBoost, as shown in Table 15.

Table 15. Comparing the performance of transfer learning against custom CNN and proposed MS-DenseNet model. See Table 4 for the explanation of metrics used in this table.

Network	***ML Model***	***Accuracy [%]***	***F1_score [%]***	***Recall [%]***	***Precision [%]***
VGG19	AdaBoost	86.2	84.9	84.7	87.8
MobileNet	XGBoost	87.7	86.9	86.7	88.3
DenseNet121	KNN	86.3	85.1	85.3	87.8
Custom CNN		83.0	76.0	65.0	93.0
Clinical interpretation		87.0	83.0	75.0	94.0
MS-DenseNet	**AdaBoost**	**97.0**	**96.0**	**96.2**	**95.2**

4.3. Performance of MS-DenseNet

It looks like the performance of the feature-extracted MS-DenseNet varies depending on the machine learning model used for classification. The AdaBoost model achieved the highest accuracy (97%) and F1 score (0.96), followed closely by the Random Forest model with an accuracy of 94.9% and F1 score of 0.903, as shown in Figure 21 and Table 16. The SVM and XGBoost models also achieved high accuracy scores, with SVM at 93.4% and XGBoost at 93.5%. However, the KNN and MLP models did not perform as well, with KNN achieving an accuracy of 81% and MLP achieving an accuracy of 78.8%.

In terms of precision and recall, the AdaBoost model achieved the highest precision and recall scores (0.952 and 0.962 respectively), followed by the Random Forest model with precision and recall scores of 0.823 and 0.958 respectively. The SVM and XGBoost models also achieved high precision and recall scores, but the KNN and MLP models did not perform as well in these areas.

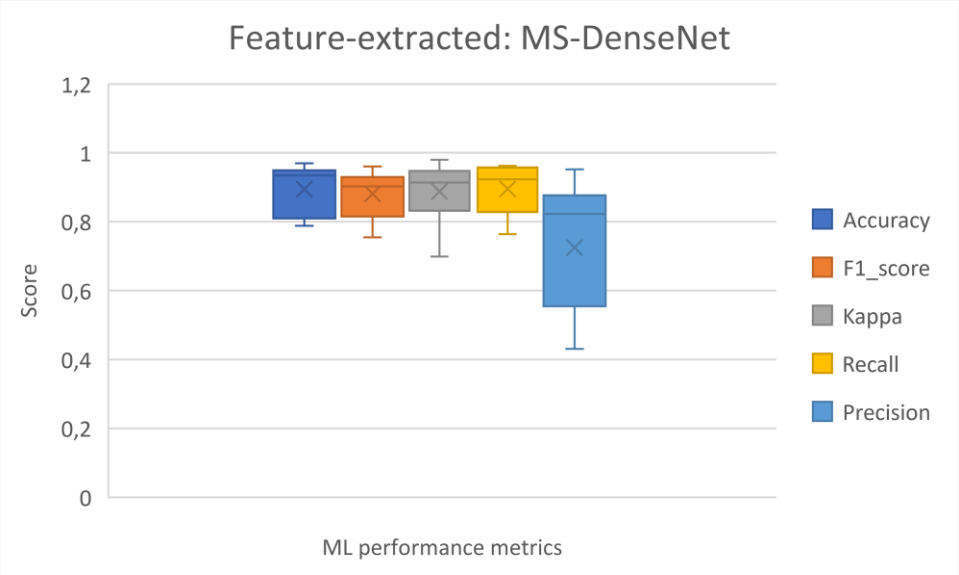

Figure 21. Evaluation metrics of MS-DenseNet. See Figure 10 for the explanation of colors and symbols used in this figure.

Table 16. Evaluation metrics of proposed model: MS-DenseNet. See Table 4 for the explanation of metrics used in this table.

Model	***Accuracy [%]***	***F1_score [%]***	***Kappa [%]***	***Recall [%]***	***Precision [%]***
SVM	93.4	92.7	94.7	92.3	85.6
Random Forest	94.9	90.3	91.4	95.8	82.3
AdaBoost	**97.0**	**96.0**	**98.0**	**96.2**	**95.2**
KNN	81.0	75.5	83.2	76.4	55.5
XGBoost	93.5	93.0	93.8	92.9	87.7
Bagging	87.7	88.2	90.4	902	58.2
MLP	78.8	81.5	69.9	82.8	43.1

Overall, the AdaBoost and Random Forest models seem to be the most effective for classification using the MS-DenseNet features, achieving high accuracy, F1 score, precision, and recall scores. The SVM and XGBoost models also show promise, while the KNN and MLP models may not be the best choice for this particular task.

5. DISCUSSION

To adapt to the new realities of the digital economy, businesses must undergo digital transformation, a key process with far-reaching consequences. Companies now must undergo digital transformations to ensure they can compete in the digital economy, and this helps with thinking about the value of data in keeping and expanding enterprises. Instead, radiology and digital transformation require the precise identification of diseases via digital imagery. Many technological challenges related to disease identification have been significantly advanced by deep learning techniques, especially CNNs.

So, we present a revolutionary lightweight architecture called MS-DenseNet, which is based on well-known mobile neural networks but has a smaller model size and improved accuracy when it comes to detecting ischemic disease in polar maps. As the backbone network, we opted for the state-of-the-art DenseNet, and we swapped out the standard convolution in dense blocks in favour of depth-separable convolution to reduce the model size and make more efficient use of the model parameters. Next, we added SE blocks into proposed network to emphasize the beneficial feature channels whilst suppressing the undesired feature channels; this made efficient use of channel interdependencies and allowed for the greatest reuse of inter-channel connections, which ultimately led to better model performance.

In our work, we presented deep feature extraction methods by using pre-trained models in order to extract features from polar map data. The extracted features are then classified by machine learning algorithms with 5-fold cross-validation. With this method, we achieved up to 87% accuracy. Moreover, this accuracy is further improved to 97% by applying proposed model MS-DenseNet which outperformed all the previously related techniques to automatically identity ischemia from polar maps, as shown in Table 1.

The experimental results demonstrate substantial efficiency advantages on patient data acquired by PET imaging. This suggests that the proposed method is superior to previous state-of-the-art deep learning models for detecting ischemia disease in polar maps and for image classification in general. We hope to refine the suggested model and increase the

accuracy with which ischemia illness can be detected in future work. We'd also wish to broaden its practical use.

6. CONCLUSION

In this thesis, we have explored the potential of transfer learning, specifically the MS-DenseNet model, to enhance the accuracy of ischemia detection from polar maps. Our proposed MS-DenseNet model has demonstrated a remarkable improvement in accuracy compared to traditional methods, achieving an impressive 97% accuracy in ischemia detection. This represents a 10% improvement over the other highest accuracy of 87% that was achieved using traditional transfer learning techniques and clinical interpretation.

Our study began with a comprehensive review of the literature on transfer learning and its applications in the field of medical imaging, particularly in ischemia detection from polar maps. We then conducted a thorough analysis of various pre-trained models and their performance in detecting ischemia. Based on this analysis, we identified the DenseNet model as a suitable foundation for our proposed MS-DenseNet model.

We developed the MS-DenseNet model by modifying the DenseNet architecture, replacing regular convolution layers with depthwise separable convolution layers and additionally incorporating SE module to highlight the useful features channels while suppressing useless feature channels. Our experimental results revealed that the MS-DenseNet model significantly outperformed traditional transfer learning methods in ischemia detection from polar maps. The model's superior performance can be attributed to its enhanced ability to capture intricate patterns and subtle differences in the images, which are essential for accurate ischemia detection.

The success of the MS-DenseNet model has important implications for clinical practice. By providing an accurate and reliable means of detecting ischemia from polar maps, our model has the potential to significantly improve patient outcomes by enabling earlier diagnosis and intervention. Moreover, the MS-DenseNet model could potentially be applied to other medical imaging tasks, further expanding its potential impact in the field of healthcare.

In conclusion, this thesis demonstrates the effectiveness of transfer learning and the MS-DenseNet model in improving the accuracy of ischemia detection from polar maps. Our findings underscore the potential of leveraging advanced deep learning techniques to enhance the capabilities of medical imaging, ultimately leading to better patient care and outcomes. Future research could explore the integration of our model into clinical workflows and its application in other medical imaging tasks to further validate and expand its potential impact.

ACKNOWLEDGEMENT

I would like to express my deepest gratitude to my parents, who have been a constant source of support, encouragement, and inspiration throughout my academic journey. Their unwavering belief in my abilities and their unconditional love has motivated me to persevere and achieve my goals. I dedicate this thesis to them, as a testament to their invaluable role in my life.

I am immensely grateful to the entire staff of the BIMA department at the Abo Akademi University and the University of Turku. The exceptional academic environment and the collaborative spirit within the department have been instrumental in my growth as a researcher. In particular, I would like to express my profound appreciation for Prof. Abdulhamit Subasi, and Prof. Riku Klen who has been exemplary mentors and supervisors at Turku PET Centre. Their expertise, dedication, and commitment to excellence have had a lasting impact on my research and professional development. Their continuous support, constructive feedback, and encouragement have been indispensable in the completion of this thesis.

I am also grateful to my fellow students and colleagues for their camaraderie, intellectual stimulation, and valuable discussions. Their contributions have enriched my academic experience and made my time at the Abo Akademi University and the University of Turku, both rewarding and enjoyable.

REFERENCES

[1] "RBC Capital Markets | Navigating the Changing Face of Healthcare Episode." https://www.rbccm.com/en/gib/healthcare/story.page (accessed Apr. 06, 2023).

[2] G. Litjens *et al.*, "A survey on deep learning in medical image analysis," *Med Image Anal*, vol. 42, pp. 60–88, Dec. 2017, doi: 10.1016/j.media.2017.07.005.

[3] "Cardiovascular disease deaths and disparities increased in 2020 | NHLBI, NIH," Jun. 28, 2021. https://www.nhlbi.nih.gov/news/2021/cardiovascular-disease-deaths-and-disparities-increased-2020 (accessed Apr. 06, 2023).

[4] R. K. Wadhera *et al.*, "Racial and Ethnic Disparities in Heart and Cerebrovascular Disease Deaths During the COVID-19 Pandemic in the United States," *Circulation*, vol. 143, no. 24, pp. 2346–2354, Jun. 2021, doi: 10.1161/CIRCULATIONAHA.121.054378.

[5] R. R. Packard, S.-C. Huang, M. Dahlbom, J. Czernin, and J. Maddahi, "Absolute quantitation of myocardial blood flow in human subjects with or without myocardial ischemia using dynamic flurpiridaz F 18 PET," *Journal of Nuclear Medicine*, vol. 55, no. 9, pp. 1438–1444, 2014.

[6] S. S. Yadav and S. M. Jadhav, "Deep convolutional neural network based medical image classification for disease diagnosis," *Journal of Big data*, vol. 6, no. 1, pp. 1–18, 2019.

[7] L. E. Juarez-Orozco, R. J. Knol, C. A. Sanchez-Catasus, O. Martinez-Manzanera, F. M. Van der Zant, and J. Knuuti, "Machine learning in the integration of simple variables for identifying patients with myocardial ischemia," *Journal of Nuclear Cardiology*, vol. 27, pp. 147–155, 2020.

[8] L. E. Juarez-Orozco, O. Martinez-Manzanera, A. E. Storti, and J. Knuuti, "Machine Learning in the Evaluation of Myocardial Ischemia Through Nuclear Cardiology," *Curr Cardiovasc Imaging Rep*, vol. 12, no. 2, p. 5, Feb. 2019, doi: 10.1007/s12410-019-9480-x.

[9] E. P. V. Le, Y. Wang, Y. Huang, S. Hickman, and F. J. Gilbert, "Artificial intelligence in breast imaging," *Clinical radiology*, vol. 74, no. 5, pp. 357–366, 2019.

[10] F. Al-Turjman, M. H. Nawaz, and U. D. Ulusar, "Intelligence in the Internet of Medical Things era: A systematic review of current and future trends," *Computer Communications*, vol. 150, pp. 644–660, Jan. 2020, doi: 10.1016/j.comcom.2019.12.030.

[11] A. Esteva *et al.*, "A guide to deep learning in healthcare," *Nature medicine*, vol. 25, no. 1, pp. 24–29, 2019.

[12] Z. Camlica, H. R. Tizhoosh, and F. Khalvati, "Medical image classification via SVM using LBP features from saliency-based folded data," in *2015 IEEE 14th international conference on machine learning and applications (ICMLA)*, IEEE, 2015, pp. 128–132.

[13] J. Zhuang, J. Cai, R. Wang, J. Zhang, and W.-S. Zheng, "Deep kNN for medical image classification," in *Medical Image Computing and Computer Assisted Intervention–MICCAI 2020: 23rd International Conference, Lima, Peru, October 4–8, 2020, Proceedings, Part I 23*, Springer, 2020, pp. 127–136.

[14] A. Krizhevsky, I. Sutskever, and G. E. Hinton, "Imagenet classification with deep convolutional neural networks," *Communications of the ACM*, vol. 60, no. 6, pp. 84–90, 2017.

[15] H.-C. Shin *et al.*, "Deep convolutional neural networks for computer-aided detection: CNN architectures, dataset characteristics and transfer learning," *IEEE transactions on medical imaging*, vol. 35, no. 5, pp. 1285–1298, 2016.

[16] R. Yamashita, M. Nishio, R. K. G. Do, and K. Togashi, "Convolutional neural networks: an overview and application in radiology," *Insights into imaging*, vol. 9, pp. 611–629, 2018.

[17] F. H. R. France, "Ethics and biomedical information," *International journal of medical informatics*, vol. 49, no. 1, pp. 111–115, 1998.

[18] C. Tan, F. Sun, T. Kong, W. Zhang, C. Yang, and C. Liu, "A survey on deep transfer learning," in *Artificial Neural Networks and Machine Learning–ICANN 2018: 27th International Conference on Artificial Neural Networks, Rhodes, Greece, October 4-7, 2018, Proceedings, Part III 27*, Springer, 2018, pp. 270–279.
[19] F. Zhuang *et al.*, "A comprehensive survey on transfer learning," *Proceedings of the IEEE*, vol. 109, no. 1, pp. 43–76, 2020.
[20] K. Weiss, T. M. Khoshgoftaar, and D. Wang, "A survey of transfer learning," *Journal of Big data*, vol. 3, no. 1, pp. 1–40, 2016.
[21] M. Shaha and M. Pawar, "Transfer learning for image classification," in *2018 second international conference on electronics, communication and aerospace technology (ICECA)*, IEEE, 2018, pp. 656–660.
[22] M. Raghu, C. Zhang, J. Kleinberg, and S. Bengio, "Transfusion: Understanding transfer learning for medical imaging," *Advances in neural information processing systems*, vol. 32, 2019.
[23] J. Teuho, J. Schultz, R. Klén, A. Saraste, N. Ono, and S. Kanaya, "Comparison of 12 Machine Learning Methods for Polar Map Classification in Cardiac Perfusion PET," in *2021 IEEE Nuclear Science Symposium and Medical Imaging Conference (NSS/MIC)*, IEEE, 2021, pp. 1–3.
[24] J. Teuho *et al.*, "Classification of ischemia from myocardial polar maps in 15O–H2O cardiac perfusion imaging using a convolutional neural network," *Scientific Reports*, vol. 12, no. 1, pp. 1–12, 2022.
[25] J. Teuho and R. Klén, "Seyedmohammadreza Hosseini".
[26] -Orozco Luis Eduardo Juarez, -Manzanera Octavio Martinez, der Z. F. M. van, R. J. J. Knol, and J. Knuuti, "Deep Learning in Quantitative PET Myocardial Perfusion Imaging," *JACC: Cardiovascular Imaging*, vol. 13, no. 1_Part_1, pp. 180–182, Jan. 2020, doi: 10.1016/j.jcmg.2019.08.009.
[27] U. R. Acharya, H. Fujita, S. L. Oh, Y. Hagiwara, J. H. Tan, and M. Adam, "Application of deep convolutional neural network for automated detection of myocardial infarction using ECG signals," *Information Sciences*, vol. 415–416, pp. 190–198, Nov. 2017, doi: 10.1016/j.ins.2017.06.027.
[28] U. R. Acharya, H. Fujita, O. S. Lih, M. Adam, J. H. Tan, and C. K. Chua, "Automated detection of coronary artery disease using different durations of ECG segments with convolutional neural network," *Knowledge-Based Systems*, vol. 132, pp. 62–71, Sep. 2017, doi: 10.1016/j.knosys.2017.06.003.
[29] R. Ross, "Cell biology of atherosclerosis," *Annual review of physiology*, vol. 57, no. 1, pp. 791–804, 1995.
[30] M. E. Widlansky, N. Gokce, J. F. Keaney, and J. A. Vita, "The clinical implications of endothelial dysfunction," *Journal of the American College of Cardiology*, vol. 42, no. 7, pp. 1149–1160, 2003.
[31] J.-K. Song, "Coronary artery vasospasm," *Korean circulation journal*, vol. 48, no. 9, pp. 767–777, 2018.
[32] B. B. Navi *et al.*, "Recurrent thromboembolic events after ischemic stroke in patients with cancer," *Neurology*, vol. 83, no. 1, pp. 26–33, 2014.
[33] M. Hauser, "Congenital anomalies of the coronary arteries," *Heart*, vol. 91, no. 9, pp. 1240–1245, 2005.
[34] D. J. Duncker, A. Koller, D. Merkus, and J. M. Canty, "Regulation of Coronary Blood Flow in Health and Ischemic Heart Disease," *Prog Cardiovasc Dis*, vol. 57, no. 5, pp. 409–422, 2015, doi: 10.1016/j.pcad.2014.12.002.

[35] P. L. da Luz, M. H. Weil, and H. Shubin, "Current concepts on mechanisms and treatment of cardiogenic shock," *American Heart Journal*, vol. 92, no. 1, pp. 103–113, 1976.
[36] D. M. Mancini, T. H. Le Jemtel, S. Factor, and E. H. Sonnenblick, "Central and peripheral components of cardiac failure," *The American Journal of Medicine*, vol. 80, no. 2, pp. 2–13, 1986.
[37] J. A. Kraut and N. E. Madias, "Treatment of acute metabolic acidosis: a pathophysiologic approach," *Nature Reviews Nephrology*, vol. 8, no. 10, pp. 589–601, 2012.
[38] G. D. Giannoglou, Y. S. Chatzizisis, and G. Misirli, "The syndrome of rhabdomyolysis: pathophysiology and diagnosis," *European journal of internal medicine*, vol. 18, no. 2, pp. 90–100, 2007.
[39] D. Garcia-Dorado, M. Ruiz-Meana, J. Inserte, A. Rodriguez-Sinovas, and H. M. Piper, "Calcium-mediated cell death during myocardial reperfusion," *Cardiovascular research*, vol. 94, no. 2, pp. 168–180, 2012.
[40] R. Bolli and E. Marbán, "Molecular and cellular mechanisms of myocardial stunning," *Physiological reviews*, vol. 79, no. 2, pp. 609–634, 1999.
[41] T. M. Scarabelli *et al.*, "Clinical implications of apoptosis in ischemic myocardium," *Current problems in cardiology*, vol. 31, no. 3, pp. 181–264, 2006.
[42] J. L. Park and B. R. Lucchesi, "Mechanisms of myocardial reperfusion injury," *The Annals of thoracic surgery*, vol. 68, no. 5, pp. 1905–1912, 1999.
[43] N. G. Frangogiannis, "The immune system and cardiac repair," *Pharmacological research*, vol. 58, no. 2, pp. 88–111, 2008.
[44] R. Lazzara and B. J. Scherlag, "Cellular electrophysiology and ischemia," *Physiology and Pathophysiology of the Heart*, pp. 493–508, 1989.
[45] H. A. Fozzard and J. C. Makielski, "The electrophysiology of acute myocardial ischemia," *Annual review of medicine*, vol. 36, no. 1, pp. 275–284, 1985.
[46] N. A. Trayanova and J. J. Rice, "Cardiac electromechanical models: from cell to organ," *Frontiers in physiology*, vol. 2, p. 43, 2011.
[47] J. M. Di Diego and C. Antzelevitch, "Ischemic ventricular arrhythmias: experimental models and their clinical relevance," *Heart Rhythm*, vol. 8, no. 12, pp. 1963–1968, 2011.
[48] I. Peate, "Caring for the patient with angina: causes and treatment," *British Journal of Healthcare Assistants*, vol. 5, no. 2, pp. 65–69, 2011.
[49] B. G. Katzung and K. Chatterjee, "12 Vasodilators & the Treatment of Angina Pectoris," *Basic & clinical pharmacology*, vol. 4, p. 140, 1989.
[50] P. F. Cohn, K. M. Fox, W. the A. of, and C. Daly, "Silent myocardial ischemia," *Circulation*, vol. 108, no. 10, pp. 1263–1277, 2003.
[51] R. S. Whelan, V. Kaplinskiy, and R. N. Kitsis, "Cell death in the pathogenesis of heart disease: mechanisms and significance," *Annual review of physiology*, vol. 72, pp. 19–44, 2010.
[52] D. Gabriel-Costa, "The pathophysiology of myocardial infarction-induced heart failure," *Pathophysiology*, vol. 25, no. 4, pp. 277–284, 2018.
[53] N. Luqman, R. J. Sung, C.-L. Wang, and C.-T. Kuo, "Myocardial ischemia and ventricular fibrillation: pathophysiology and clinical implications," *International journal of cardiology*, vol. 119, no. 3, pp. 283–290, 2007.
[54] A. R. Patel and C. M. Kramer, "Role of cardiac magnetic resonance in the diagnosis and prognosis of nonischemic cardiomyopathy," *JACC: Cardiovascular Imaging*, vol. 10, no. 10 Part A, pp. 1180–1193, 2017.
[55] I. S. Syed *et al.*, "Role of cardiac magnetic resonance imaging in the detection of cardiac amyloidosis," *JACC: cardiovascular imaging*, vol. 3, no. 2, pp. 155–164, 2010.

[56] S. Gargiulo *et al.*, "PET/CT imaging in mouse models of myocardial ischemia," *Journal of Biomedicine and Biotechnology*, vol. 2012, 2012.
[57] M. D. Cerqueira, G. D. Harp, and J. L. Ritchie, "Evaluation of myocardial perfusion and function by single photon emission computed tomography," in *Seminars in nuclear medicine*, Elsevier, 1987, pp. 200–213.
[58] K. K. Kumamaru, B. E. Hoppel, R. T. Mather, and F. J. Rybicki, "CT angiography: current technology and clinical use," *Radiologic Clinics*, vol. 48, no. 2, pp. 213–235, 2010.
[59] U. Hoffmann, M. Ferencik, R. C. Cury, and A. J. Pena, "Coronary CT angiography," *Journal of nuclear medicine*, vol. 47, no. 5, pp. 797–806, 2006.
[60] R. Olszewski *et al.*, "The clinical applications of contrast echocardiography," *European Journal of Echocardiography*, vol. 8, no. 3, pp. s13–s23, 2007.
[61] B. P. Davidson and J. R. Lindner, "Future applications of contrast echocardiography," *Heart*, vol. 98, no. 3, pp. 246–253, 2012.
[62] K. S. Mehta, J. J. Lee, A. A. Taha, E. Avgerinos, and R. A. Chaer, "Vascular applications of contrast-enhanced ultrasound imaging," *Journal of vascular surgery*, vol. 66, no. 1, pp. 266–274, 2017.
[63] F. Hayes-Roth, "Rule-based systems," *Commun. ACM*, vol. 28, no. 9, pp. 921–932, Sep. 1985, doi: 10.1145/4284.4286.
[64] M. I. Jordan and T. M. Mitchell, "Machine learning: Trends, perspectives, and prospects," *Science*, vol. 349, no. 6245, pp. 255–260, 2015.
[65] A. Shrestha and A. Mahmood, "Review of Deep Learning Algorithms and Architectures," *IEEE Access*, vol. 7, pp. 53040–53065, 2019, doi: 10.1109/ACCESS.2019.2912200.
[66] J. Hirschberg and C. D. Manning, "Advances in natural language processing," *Science*, vol. 349, no. 6245, pp. 261–266, 2015.
[67] K.-H. Yu, A. L. Beam, and I. S. Kohane, "Artificial intelligence in healthcare," *Nature biomedical engineering*, vol. 2, no. 10, pp. 719–731, 2018.
[68] C. Combi and G. Pozzi, "Clinical information systems and artificial intelligence: recent research trends," *Yearbook of medical informatics*, vol. 28, no. 01, pp. 083–094, 2019.
[69] R. Manne and S. C. Kantheti, "Application of artificial intelligence in healthcare: chances and challenges," *Current Journal of Applied Science and Technology*, vol. 40, no. 6, pp. 78–89, 2021.
[70] R. Antel, S. Abbasgholizadeh-Rahimi, E. Guadagno, J. M. Harley, and D. Poenaru, "The use of artificial intelligence and virtual reality in doctor-patient risk communication: A scoping review," *Patient Education and Counseling*, 2022.
[71] E. Chikhaoui, A. Alajmi, and S. Larabi-Marie-Sainte, "Artificial intelligence applications in healthcare sector: Ethical and legal challenges," *Emerging Science Journal*, vol. 6, no. 4, pp. 717–738, 2022.
[72] V. Nasteski, "An overview of the supervised machine learning methods," *Horizons. b*, vol. 4, pp. 51–62, 2017.
[73] M. Alloghani, D. Al-Jumeily, J. Mustafina, A. Hussain, and A. J. Aljaaf, "A systematic review on supervised and unsupervised machine learning algorithms for data science," *Supervised and unsupervised learning for data science*, pp. 3–21, 2020.
[74] E. Akanksha, N. Sharma, and K. Gulati, "Review on reinforcement learning, research evolution and scope of application," in *2021 5th international conference on computing methodologies and communication (ICCMC)*, IEEE, 2021, pp. 1416–1423.
[75] "AlphaGo." https://www.deepmind.com/research/highlighted-research/alphago (accessed Apr. 27, 2023).

[76] J. Yanase and E. Triantaphyllou, "A systematic survey of computer-aided diagnosis in medicine: Past and present developments," *Expert Systems with Applications*, vol. 138, p. 112821, 2019.
[77] F. Lopez-Jimenez *et al.*, "Artificial intelligence in cardiology: present and future," in *Mayo Clinic Proceedings*, Elsevier, 2020, pp. 1015–1039.
[78] J. Dekhtiar, A. Durupt, M. Bricogne, B. Eynard, H. Rowson, and D. Kiritsis, "Deep learning for big data applications in CAD and PLM–Research review, opportunities and case study," *Computers in Industry*, vol. 100, pp. 227–243, 2018.
[79] Q. Li, W. Cai, X. Wang, Y. Zhou, D. D. Feng, and M. Chen, "Medical image classification with convolutional neural network," in *2014 13th international conference on control automation robotics & vision (ICARCV)*, IEEE, 2014, pp. 844–848.
[80] G. Farias *et al.*, "Automatic feature extraction in large fusion databases by using deep learning approach," *Fusion Engineering and Design*, vol. 112, pp. 979–983, 2016.
[81] I. Saritas, "Prediction of breast cancer using artificial neural networks," *Journal of Medical Systems*, vol. 36, pp. 2901–2907, 2012.
[82] E. Westman, J.-S. Muehlboeck, and A. Simmons, "Combining MRI and CSF measures for classification of Alzheimer's disease and prediction of mild cognitive impairment conversion," *Neuroimage*, vol. 62, no. 1, pp. 229–238, 2012.
[83] M. H. Hesamian, W. Jia, X. He, and P. Kennedy, "Deep learning techniques for medical image segmentation: achievements and challenges," *Journal of digital imaging*, vol. 32, pp. 582–596, 2019.
[84] Z. Naaqvi, S. Akbar, S. A. Hassan, and Q. U. Ain, "Detection of Liver Cancer through Computed Tomography Images using Deep Convolutional Neural Networks," in *2022 2nd International Conference on Digital Futures and Transformative Technologies (ICoDT2)*, IEEE, 2022, pp. 1–6.
[85] M. M. Najafabadi, F. Villanustre, T. M. Khoshgoftaar, N. Seliya, R. Wald, and E. Muharemagic, "Deep learning applications and challenges in big data analytics," *Journal of big data*, vol. 2, no. 1, pp. 1–21, 2015.
[86] I. Guyon and A. Elisseeff, "An introduction to feature extraction," *Feature extraction: foundations and applications*, pp. 1–25, 2006.
[87] L. Torrey and J. Shavlik, "Transfer learning," in *Handbook of research on machine learning applications and trends: algorithms, methods, and techniques*, IGI global, 2010, pp. 242–264.
[88] Y. H. Liu, "Feature extraction and image recognition with convolutional neural networks," in *Journal of Physics: Conference Series*, IOP Publishing, 2018, p. 062032.
[89] X. Jiang, "Feature extraction for image recognition and computer vision," in *2009 2nd IEEE international conference on computer science and information technology*, IEEE, 2009, pp. 1–15.
[90] G. Sharma, K. Umapathy, and S. Krishnan, "Trends in audio signal feature extraction methods," *Applied Acoustics*, vol. 158, p. 107020, 2020.
[91] J. C. M. Serrano, O. Papakyriakopoulos, and S. Hegelich, "NLP-based feature extraction for the detection of COVID-19 misinformation videos on YouTube," in *Proceedings of the 1st Workshop on NLP for COVID-19 at ACL 2020*, 2020.
[92] M. Shaha and M. Pawar, "Transfer learning for image classification," in *2018 second international conference on electronics, communication and aerospace technology (ICECA)*, IEEE, 2018, pp. 656–660.
[93] Kriti, J. Virmani, and R. Agarwal, "Deep feature extraction and classification of breast ultrasound images," *Multimedia Tools and Applications*, vol. 79, pp. 27257–27292, 2020.

[94] A. Cichocki, "Unsupervised learning algorithms and latent variable models: PCA/SVD, CCA/PLS, ICA, NMF, etc.," in *Academic Press Library in Signal Processing*, Elsevier, 2014, pp. 1151–1238.
[95] S. Niu, Y. Liu, J. Wang, and H. Song, "A decade survey of transfer learning (2010–2020)," *IEEE Transactions on Artificial Intelligence*, vol. 1, no. 2, pp. 151–166, 2020.
[96] O. A. Montesinos López, A. Montesinos López, and J. Crossa, "Overfitting, Model Tuning, and Evaluation of Prediction Performance," in *Multivariate statistical machine learning methods for genomic prediction*, Springer, 2022, pp. 109–139.
[97] A. Gulli and S. Pal, *Deep learning with Keras*. Packt Publishing Ltd, 2017.
[98] P. S. Janardhanan, "Project repositories for machine learning with TensorFlow," *Procedia Computer Science*, vol. 171, pp. 188–196, 2020.
[99] K. Team, "Keras documentation: Keras Applications." https://keras.io/api/applications/ (accessed Apr. 27, 2023).
[100] G. Huang, D. Chen, T. Li, F. Wu, L. Van Der Maaten, and K. Q. Weinberger, "Multi-scale dense networks for resource efficient image classification," *arXiv preprint arXiv:1703.09844*, 2017.
[101] G. Huang, Z. Liu, G. Pleiss, L. Van Der Maaten, and K. Q. Weinberger, "Convolutional networks with dense connectivity," *IEEE transactions on pattern analysis and machine intelligence*, vol. 44, no. 12, pp. 8704–8716, 2019.
[102] J. Xie, N. He, L. Fang, and P. Ghamisi, "Multiscale Densely-Connected Fusion Networks for Hyperspectral Images Classification," *IEEE Transactions on Circuits and Systems for Video Technology*, vol. 31, no. 1, pp. 246–259, Jan. 2021, doi: 10.1109/TCSVT.2020.2975566.
[103] R. Zhang, F. Zhu, J. Liu, and G. Liu, "Depth-wise separable convolutions and multi-level pooling for an efficient spatial CNN-based steganalysis," *IEEE Transactions on Information Forensics and Security*, vol. 15, pp. 1138–1150, 2019.
[104] J. Chen, A. Zeb, S. Yang, D. Zhang, and Y. A. Nanehkaran, "Automatic identification of commodity label images using lightweight attention network," *Neural Computing and Applications*, vol. 33, no. 21, pp. 14413–14428, 2021.
[105] F. Chollet, "Xception: Deep learning with depthwise separable convolutions," in *Proceedings of the IEEE conference on computer vision and pattern recognition*, 2017, pp. 1251–1258.
[106] C.-F. Wang, "A Basic Introduction to Separable Convolutions," *Medium*, Aug. 14, 2018. https://towardsdatascience.com/a-basic-introduction-to-separable-convolutions-b99ec3102728 (accessed May 24, 2023).
[107] J. Hu, L. Shen, and G. Sun, "Squeeze-and-excitation networks," in *Proceedings of the IEEE conference on computer vision and pattern recognition*, 2018, pp. 7132–7141.
[108] A. F. Agarap, "Deep learning using rectified linear units (relu)," *arXiv preprint arXiv:1803.08375*, 2018.
[109] I. Stenström *et al.*, "Frequency and angiographic characteristics of coronary microvascular dysfunction in stable angina: a hybrid imaging study," *European Heart Journal-Cardiovascular Imaging*, vol. 18, no. 11, pp. 1206–1213, 2017.
[110] H. Xue, Q. Yang, and S. Chen, "SVM: Support vector machines," in *The top ten algorithms in data mining*, Chapman and Hall/CRC, 2009, pp. 51–74.
[111] Y. Ma and G. Guo, *Support vector machines applications*, vol. 649. Springer, 2014.
[112] A.-L. Boulesteix, S. Janitza, J. Kruppa, and I. R. König, "Overview of random forest methodology and practical guidance with emphasis on computational biology and bioinformatics," *Wiley Interdisciplinary Reviews: Data Mining and Knowledge Discovery*, vol. 2, no. 6, pp. 493–507, 2012.

[113] K. Fawagreh, M. M. Gaber, and E. Elyan, "Random forests: from early developments to recent advancements," *Systems Science & Control Engineering: An Open Access Journal*, vol. 2, no. 1, pp. 602–609, 2014.
[114] R. E. Schapire, "Explaining adaboost," *Empirical Inference: Festschrift in Honor of Vladimir N. Vapnik*, pp. 37–52, 2013.
[115] C. Ying, M. Qi-Guang, L. Jia-Chen, and G. Lin, "Advance and prospects of AdaBoost algorithm," *Acta Automatica Sinica*, vol. 39, no. 6, pp. 745–758, 2013.
[116] G. Guo, H. Wang, D. Bell, Y. Bi, and K. Greer, "KNN model-based approach in classification," in *On The Move to Meaningful Internet Systems 2003: CoopIS, DOA, and ODBASE: OTM Confederated International Conferences, CoopIS, DOA, and ODBASE 2003, Catania, Sicily, Italy, November 3-7, 2003. Proceedings*, Springer, 2003, pp. 986–996.
[117] V. Moghtadaiee and A. G. Dempster, "Determining the best vector distance measure for use in location fingerprinting," *Pervasive and Mobile Computing*, vol. 23, pp. 59–79, 2015.
[118] S. B. Kotsiantis, I. Zaharakis, and P. Pintelas, "Supervised machine learning: A review of classification techniques," *Emerging artificial intelligence applications in computer engineering*, vol. 160, no. 1, pp. 3–24, 2007.
[119] T. Chen *et al.*, "Xgboost: extreme gradient boosting," *R package version 0.4-2*, vol. 1, no. 4, pp. 1–4, 2015.
[120] M. Alabadla *et al.*, "Systematic review of using machine learning in imputing missing values," *IEEE Access*, 2022.
[121] T.-H. Lee, A. Ullah, and R. Wang, "Bootstrap aggregating and random forest," *Macroeconomic forecasting in the era of big data: Theory and practice*, pp. 389–429, 2020.
[122] H. Taud and J. F. Mas, "Multilayer perceptron (MLP)," *Geomatic approaches for modeling land change scenarios*, pp. 451–455, 2018.
[123] M.-C. Popescu, V. E. Balas, L. Perescu-Popescu, and N. Mastorakis, "Multilayer perceptron and neural networks," *WSEAS Transactions on Circuits and Systems*, vol. 8, no. 7, pp. 579–588, 2009.